A Decade of Death and Other Dynamics: Deepening Perspectives on the Diversity and Distribution of Sea Stars and Wasting

Michael N Dawson[1,*], Paige J. Duffin[2], Melina Giakoumis[3,†], Lauren M. Schiebelhut[1], Rodrigo Beas-Luna[4], Keith L. Bosley[5], Rita Castilho[6], Christine Ewers-Saucedo[7], Katie A. Gavenus[8], Aimee Keller[5], Brenda Konar[9], John L. Largier[10], Julio Lorda[11], C. Melissa Miner[12], Monica M. Moritsch[12], Sergio A. Navarrete[13], Sarah B. Traiger[14], Mo S. Turner[15], and John P. Wares[2,16]

[1] Life and Environmental Sciences, University of California, Merced, California 95343
[2] Department of Genetics, University of Georgia, Athens, Georgia 30602
[3] Graduate Center, City University of New York, New York 10016
[4] Universidad Autónoma de Baja California, Facultad de Ciencias Marinas, Baja California 22760, Mexico
[5] Fishery Resource Analysis and Monitoring Division, Northwest Fisheries Science Center, National Marine Fisheries Service, National Oceanic and Atmospheric Administration, Seattle, Washington 98112
[6] University of Algarve and Center for Marine Sciences, Gambelas Campus, 8005-139 Faro, Portugal
[7] Zoological Museum of the Christian-Albrechts University, Kiel, Germany
[8] Center for Alaskan Coastal Studies, Homer, Alaska 99603
[9] College of Fisheries and Ocean Sciences, University of Alaska, Fairbanks, Alaska 99775
[10] Bodega Marine Laboratory, Coastal and Marine Sciences Institute, University of California–Davis, Bodega Bay, California 94923
[11] Universidad Autónoma de Baja California, Facultad de Ciencias, Baja California 22760, Mexico
[12] Department of Ecology and Evolution, University of California, Santa Cruz, California 95060
[13] Estación Costera de Investigaciones Marinas, Las Cruces, Departamento de Ecología, Coastal Socio-Ecological Millennium Institute (SECOS), and Center for Oceanography COPAS COASTAL, Millennium Nucleus for Ecology and Conservation of Temperate Mesophotic Reef Ecosystems (NUTME), Pontificia Universidad Católica de Chile, Las Cruces, Chile
[14] US Geological Survey, Alaska Science Center, Juneau Alaska 99801
[15] Department of Biology, University of Washington, Seattle, Washington 98195
[16] Odum School of Ecology, University of Georgia, Athens, Georgia 30602

Abstract

Mass mortality events provide valuable insight into biological extremes and also ecological interactions more generally. The sea star wasting epidemic that began in 2013 catalyzed study of the microbiome, genetics, population dynamics, and community ecology of several high-profile species inhabiting the northeastern Pacific but exposed a dearth of information on the diversity, distributions, and impacts of sea star wasting for many lesser-known sea stars and a need for integration across scales. Here, we combine datasets from single-site to coast-wide studies, across time lines from weeks to decades, for 65 species. We evaluated the impacts of abiotic characteristics hypothetically associated with sea star wasting (sea surface

Received 23 July 2021; Accepted 17 September 2023; Published online 22 December 2023.
* Corresponding author; email: mdawson@ucmerced.edu.
† Present address: Institute for Comparative Genomics at the American Museum of Natural History, New York, New York, 10024.
Abbreviations: BUI, Bakun upwelling index; CPUE, catch-per-unit-effort; NMFS, National Marine Fisheries Service; SST, sea surface temperature; SSW, sea star wasting.
Online enhancement: appendix.

The Biological Bulletin, June 2023, volume 244, number 3: 143–163. https://doi.org/10.1086/727969

temperature, pelagic primary productivity, upwelling wind forcing, wave exposure, freshwater runoff) and species characteristics (depth distribution, developmental mode, diet, habitat, reproductive period). We find that the 2010s sea star wasting outbreak clearly affected a little over a dozen species, primarily intertidal and shallow subtidal taxa, causing instantaneous wasting prevalence rates of 5%–80%. Despite the collapse of some populations within weeks, environmental and species variation protracted the outbreak, which lasted 2–3 years from onset until declining to chronic background rates of 2% sea star wasting prevalence. Recruitment began immediately in many species, and in general, sea star assemblages trended toward recovery; however, recovery was heterogeneous, and a marine heatwave in 2019 raised concerns of a second decline. The abiotic stressors most associated with the 2010s sea star wasting outbreak were elevated sea surface temperature and low wave exposure, as well as freshwater discharge in the north. However, detailed data speaking directly to the biological, ecological, and environmental cause(s) and consequences of the sea star wasting outbreak remain limited in scope, unavoidably retrospective, and perhaps always indeterminate. Redressing this shortfall for the future will require a broad spectrum of monitoring studies not less than the taxonomically broad cross-scale framework we have modeled in this synthesis.

Introduction

A decade after one of the largest marine mass mortalities on record, we are still at a loss as to the cause(s) and mechanism(s) that manifested in the sea star wasting (SSW) epidemic of the early to mid-2010s. This mass-mortality event captured public and research attention because of its broad community impacts (*e.g.*, McPherson *et al.*, 2021), its inferred taxonomic breadth (Hewson *et al.*, 2014), and its severity for some taxa. Notably, it led to International Union for Conservation of Nature listing of the sunflower sea star, *Pycnopodia helianthoides*, as critically endangered (Gravem *et al.*, 2021). In addition to extirpating *P. helianthoides* from half of its range (Harvell *et al.*, 2019; Gravem *et al.*, 2021; Hamilton *et al.*, 2021), SSW decimated *Pisaster ochraceus* (Miner *et al.*, 2018), decreased the abundances of *Leptasterias* (Jaffe *et al.*, 2019), and was reported to have affected "at least 20" species (Hewson *et al.*, 2014) that span much of the asteroid tree of life (Schiebelhut *et al.*, 2022b). This was not the first SSW outbreak (*e.g.*, Dungan *et al.*, 1982; Eckert *et al.*, 2000) but is widely acknowledged to have been the most severe on record (Harvell *et al.*, 2019; Hewson *et al.*, 2019). The broad geographic and phylogenetic reach of SSW tended to focus attention toward the large scale of the catastrophe and on studies of the most affected species to determine causes and consequences. Yet the severity and timing of mass mortalities were spatially and taxonomically heterogeneous (Menge *et al.*, 2016; Montecino-Latorre *et al.*, 2016; Konar *et al.*, 2019), leading to a kaleidoscope of results and a shifting mosaic of data that has confounded clear associations between causes and effects of SSW and abiotic and biotic variation.

The hypothesized cause(s) of the 2010s SSW outbreak are diverse. The outbreak has been associated with, in chronological order of publication, a viral pathogen (Hewson *et al.*, 2014; Fuess *et al.*, 2015; Bucci *et al.*, 2017), warmer temperature (Eisenlord *et al.*, 2016; Kohl *et al.*, 2016; Harvell *et al.*, 2019), cooler temperature (Menge *et al.*, 2016), possibly reduced precipitation (Hewson *et al.*, 2018), and/or interactions thereof. The occurrence of SSW appears to have been mediated by oceanographic conditions (Aalto *et al.*, 2020) and modulated by individual size (Eisenlord *et al.*, 2016; Menge *et al.*, 2016) and genotype (Schiebelhut *et al.*, 2018). Most recently, dysoxia-induced dysbiosis was suggested as a proximate cause for SSW, with origins in excess organic matter liberated through increased primary productivity or mortality (Aquino *et al.*, 2021). These attributes of the 2010s outbreak often resemble hypothesized causes and dynamics of previous SSW outbreaks, which also implicated one or more factors possibly interacting. For example, Bates *et al.* (2009) found that SSW associated with increased temperature and was exacerbated by shelter; lesions were enriched with a ciliate and bacteria (Bates *et al.*, 2009). Dungan *et al.* (1982) likewise considered elevated temperature of primary importance but also noted extreme low salinities due to heavy rains as potential causes for SSW that devastated intertidal and shallow subtidal (intertidal/shallow subtidal) sea star populations in the Gulf of California. They considered similar die-offs in geographically and oceanographically distinct regions to indicate a common cause, ruling out most kinds of localized disturbance as potential explanations (Dungan *et al.*, 1982).

The increasing number of SSW events has not been matched by increased understanding; rather, it has emphasized persistent questions and gaps in knowledge. For example: Is temperature the primary determinant? Does it interact with other factors? Is a pathogen involved? If yes, what is it (Dungan *et al.*, 1982; Hewson *et al.*, 2018)? Information about SSW events is fragmented as a result of mismatches in the scales of events and measurements, the greater ease of sampling some taxa over others, the challenges of sampling in geographically and/or technologically remote locations, and the inevitable time and procedural constraints of in-person fieldwork. Consequently, baseline conditions, new incidences of the disease, the earliest stages of propagation, and its severity are rarely documented. This problem of piecemeal information when a geographically and taxonomically integrative picture is needed is not new (Orr *et al.*, 2020) and requires that we look beyond the immediate event to find broader understanding (Huey and Grant, 2020). This includes asking what SSW can reveal about the ecology and environment of sea stars generally and the way we study them, in addition to better understanding sea stars'

dynamics in the specific context of SSW outbreaks. Our goal here is to synthesize information from a diversity of sources, only some of which were collected in the immediate context of SSW, that describe ecological and environmental dynamics for many taxa spanning a range of spatial and temporal scales. Our objectives are to better delimit the spatial, taxonomic, and temporal influence of—and thereby better focus information on the environmental factors (agnostic of whether a pathogen was involved) possibly contributing to—SSW. The key stage in this process is to first expand analyses to consider a suite of mostly lesser-known species.

Materials and Methods

Broadscale analyses

Our goal was to summarize data for environmental variables and for each sea star species annually into half-degree latitudinal cells (aka "cell"; Fig. 1a [generated using the oce v1.4-0 (Kelley and Richards, 2021) and sf v0.9-7 (Pebesma, 2018) packages in R (R Core Team, 2020)]) or their approximate equivalent (*i.e.*, ~55–70 km; Supplementary Document 1 [Supplementary Documents 1–8 are available online]) where the coast does not run predominantly north-south.

Environment

We considered five abiotic attributes that previously have been highlighted as possibly associated with SSW: temperature, pelagic primary productivity, upwelling, wave exposure, and precipitation. The indices we used to represent these attributes, and how they were calculated, are as follows.

Temperature. We calculated a monthly sea surface temperature (SST) anomaly from monthly mean satellite data averaged over half-degree alongshore distances. The original 5-km-resolution data were downloaded from the "SST and SST Anomaly, NOAA Global Coral Bleaching Monitoring, 5km, V.3.1, Monthly, 1985–Present" dataset at National Oceanic and Atmospheric Administration Environmental Research Division Data Access Program (NOAA ERDDAP; https://coastwatch.pfeg.noaa.gov/erddap/griddap/NOAA_DHW_monthly.html), using the "griddap" function to request specific coordinate pairs from the SST gridded dataset (Supplementary Document 2). Anomalies were calculated for each cell and each of the 120 months from 2011 to 2020 by subtracting a long-term monthly average value for that cell (calculated over years 2003–2020) from the observed monthly mean temperature.

Pelagic primary productivity. We calculated a monthly mean sea surface chlorophyll *a* (Chl *a*) anomaly as an index of phytoplankton productivity within ~4 km of shore; Chl *a* satellite data were downloaded from the "Chlorophyll-a, Aqua MODIS, NPP, L3SMI, Global, 4km, Science Quality, 2003–present (Monthly Composite)" dataset at NOAA ERDDAP (https://coastwatch.pfeg.noaa.gov/erddap/griddap/erdMH1chlamday.html). The half-degree monthly anomalies were then calculated as described for SST.

Upwelling. We indexed the intensity of upwelling by using the Bakun upwelling index (BUI), which quantifies the regional shelf-scale strength of wind forcing; BUI datasets provide 6-hourly data at 15 stations, at 3° latitude intervals, along the US west coast. These were downloaded from NOAA ERDDAP (see Supplementary Document Table S2), monthly averaged and linearly interpolated to obtain values at 1° latitude resolution. The monthly anomaly was then calculated as described for SST and Chl *a*.

Wave exposure. Wave data collected every minute were downloaded from NOAA's National Data Buoy Center for 10 outercoast sites between 32.5° N and 58° N (Supplementary Document 2). For each site, wave height data were averaged hourly and then again daily (*i.e.*, a mean-of-means) to enable identification of the 75th percentile of the daily wave heights as an index of monthly exposure to large waves in each region. Although local-scale variability is not captured, seasonal and interannual differences are well represented and these offshore sites index significant alongshore distances (similar in scale to other 1° indices).

Freshwater runoff. As an index for freshwater influences in the coastal ocean, we used river flow rates for 18 selected coastal drainages between Alaska and southern California (note we excluded large drainage systems that are not representative of variability in near-coast precipitation or near-coast salinity effects, *e.g.*, Columbia River). While flow rates varied markedly between rivers, each provided an index identifying times of high or low runoff as representative for proximate rivers and creeks. These data were downloaded from the US Geological Survey National Water Information System (see Supplementary Document 2). Flow data were averaged monthly and normalized by dividing each monthly observation by the long-term monthly average for that site (calculated from data spanning 2003–2020).

Biology

We censused 18 teams surveying sea stars in the northeastern Pacific, of which six contributed datasets: MexCal (Beas-Luna *et al.*, 2020), Center for Alaskan Coastal Studies (K. Gavenus), Ocean Wise, the Multi-Agency Rocky Intertidal Network (MARINe, 2015; Miner *et al.*, 2018), National Marine Fisheries Service (NMFS; Keller *et al.*, 2017), and Gulf Watch Alaska (Dean and Bodkin, 2011; Dean *et al.*, 2014; Konar *et al.*, 2019; USGS, 2022). Datasets spanned from southern Baja California to the northern Gulf of Alaska and from the intertidal zone to 1430-m depth, and they included up to four basic data types: occurrence, abundance, SSW prevalence, and number of recruits. Because different datasets used different methods (*e.g.*, trawls providing catch-per-unit-effort [CPUE], transects providing densities, and counts in permanent plots;

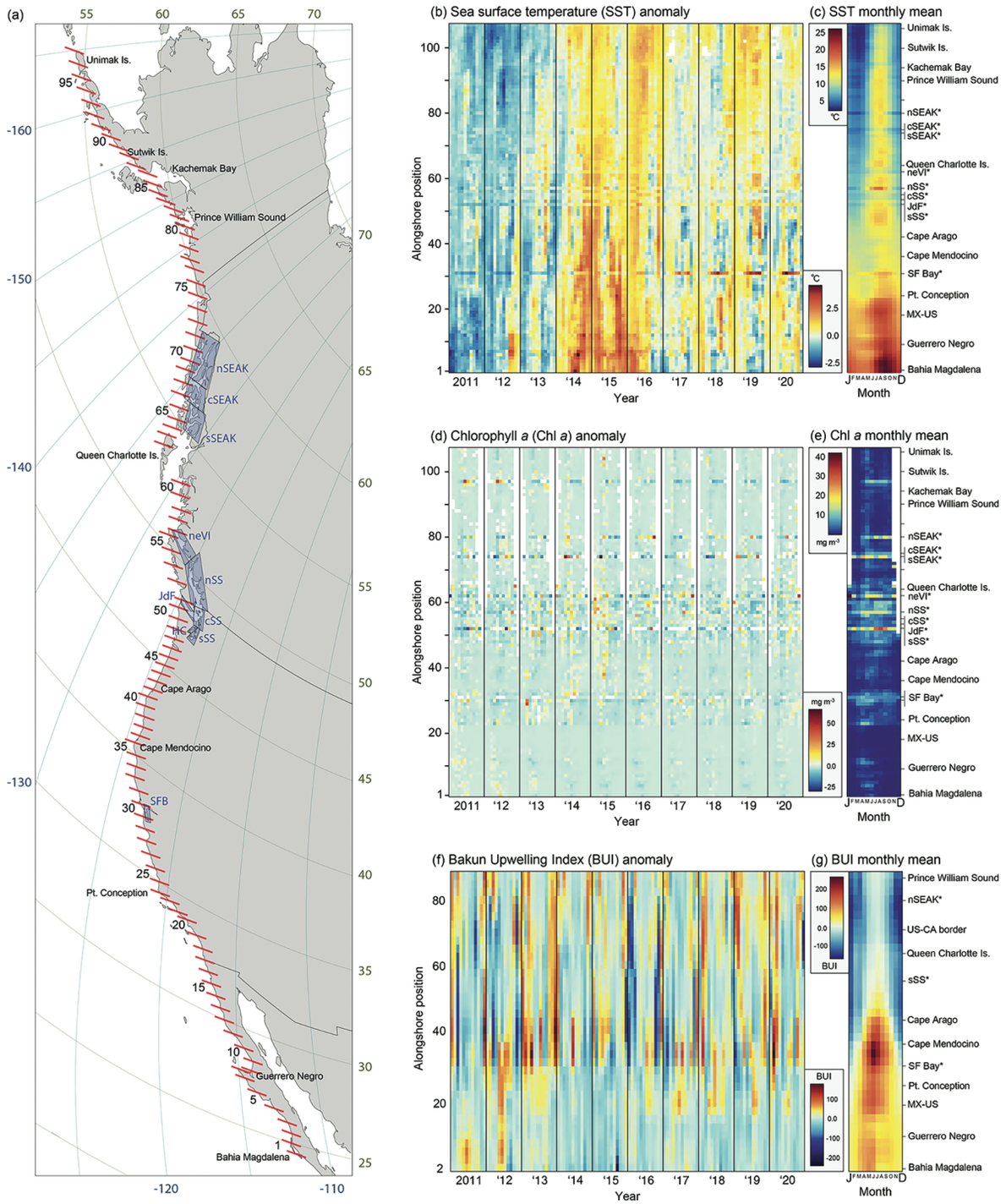

Figure 1. Study design for sea star surveys and complementary large-scale spatial and temporal environmental variation, 2011–2020. (a) Map showing the extent and resolution of sea star survey data compiled for this study. The red crosshairs show consecutive boundaries of latitudinal cells used to aggregate data; they are numbered consecutively and labeled periodically from south to northwest along the outer coast. Divisions of inshore waters around San Francisco (SFB), Puget Sound and Vancouver Island (sSS, southern Salish Sea; HC, Hood Canal; cSS, central Salish Sea; JdF, Strait of Juan de Fuca; nSS, northern Salish Sea; neVI, northeastern Vancouver Island), and southeastern Alaska (SEAK; sSEAK, southern; cSEAK, central; nSEAK, northern) are bounded by boxes. The map is an azimuthal equidistant projection. Sea surface temperature (SST) monthly anomaly (b) and SST monthly climatology (c) for 2003–2020. Chlorophyll *a* (Chl *a*) monthly anomaly (d) and Chl *a* monthly climatology (e) for 2003–2020; white cells indicate missing data due primarily to absence of daylight at high latitudes during northern hemisphere winter. Bakun upwelling index (BUI) monthly anomaly (f) and BUI monthly climatology (g) for 2003–2020. Asterisks indicate the divisions of inshore waters around San Francisco, Puget Sound and Vancouver Island, and southeastern Alaska, whereas other sites indicate outer coastal regions. Place names are provided to match sea star and environmental datasets, for which numbering systems differ in resolution.

see detailed methods in Supplementary Document 3) and included different numbers of sites and intensities of sampling, we used the following procedure for data harmonization.

Species' occurrence. If a species was documented in any of the seven datasets, at any latitudinal point in the study area (Fig. 1), in a given year, the species was coded as present. A "pre-SSW" ("pre-2013") reference point was limited to considering data from 2000 to 2012, to avoid inclusion of very rare species, which were only historically (pre-2000) present in the study area. Species were coded as absent only if there was an effort to sample them in one or more surveys and they were not found; if no effort was documented to sample a species, it was coded as "No Data" for that year.

Species' abundance. Considering each dataset separately, we standardized each species × cell value by rescaling the annual abundances as proportions of the maximum abundance observed for that species in that time series; the highest recorded annual abundance for each species was therefore plotted as 1 and the lowest abundance a fraction thereof, with the minimum possible being 0 when species were absent. Time series with an observation in only one year were excluded, because that value could not be standardized relative to any other measurement and so would inevitably be 1. Pre-2013 data were calculated as an average of data between 2006 and 2012. For any species × cell combinations that were represented in more than one dataset, we then calculated the mean relative abundance for each cell × year. Because some new sites added in 2017 or more recently disproportionately had zero abundances, we calculated the mean relative abundance both including and excluding zeros to assess the possibility that zeros were driving observed patterns.

Severity of SSW. A subset of intertidal datasets assessed either (*a*) presence/absence of wasting disease or (*b*) percent prevalence, that is, proportion of observed sea stars that were symptomatic. To report trends by species, (*a*) SSW occurrence data were summed and (*b*) prevalence data were averaged, across all datasets and latitudinal cells for each species annually. To report trends by latitude, (*a*) SSW occurrence data were summed and (*b*) prevalence data were averaged, across all datasets and all species for each latitudinal cell annually.

Recruitment. Two datasets provided estimates of the number of recruits. For intertidal *Pisaster ochraceus* (Brandt, 1835) and *Evasterias troschelii* (Stimpson, 1862), individuals <30 mm radius were considered recently recruited in the preceding year (Miner *et al.*, 2018), though other studies have used smaller cutoffs for identifying the past year's recruits; for example, Menge *et al.* (2016) used <50 mm diameter. For subtidal surveys, individuals with radius <50 mm were considered recent recruits. These choices trade off being overly inclusive *versus* overly exclusive of actual recruits.

For display, these data were then organized primarily by latitude or by species' depth distributions, the order being based on the median depth of species occurrences in the included datasets. From the four basic datasets, we aimed to infer three additional attributes.

Number of species affected (*i.e.*, those that were extirpated, declined dramatically in abundance, and/or had high frequencies of symptoms of wasting). Records for intertidal surveys commonly include observations of SSW. By contrast, SSW has not been recorded as part of NMFS trawl surveys. As such, we analyzed species' abundance trends through time to determine which of these species declined during the high wasting period 2013–2015 in California, Oregon, and Washington and to categorize those impacted into degrees of severity. We plotted the mean and 95% confidence interval (CI) for each species that had ≥0.01 mean CPUE for the period 2006–2012 (data collected 2003–2005 were not reliably identified to species) and calculated the mean CPUE for each year 2013–2018. Species were then categorized as (1) decreasing if the post-2012 annual means fell below the 2006–2012 lower 95% CI for two or more consecutive years starting between 2013 and 2015, (2) increasing if the post-2012 annual means rose above the 2006–2012 upper 95% CI for three consecutive or four nonconsecutive years starting between 2013 and 2015, or (3) no change if the species' abundance trend did not fit either of the two preceding categories.

Timing of onset of the SSW outbreak. We examined for unusual declines in species' abundances and elevated or peak levels of SSW to delimit the start of the SSW outbreak.

Timing of the end of the SSW outbreak. We examined for increases in affected species' abundances, increases in recruitment, and declines in the prevalence of symptomatic sea stars to delimit the end of the SSW outbreak.

Small-scale analyses

Time line of SSW progression. Intertidal *P. ochraceus* were surveyed every 2 weeks at 10 sites across the San Juan Islands, Washington, in 2014 (May–August; San Juan, Orcas, and Lopez Islands). There were 1–4 (mean = 2.4; median = 3) fixed plots per site, ranging in size from 3.3 to 102 m in length (mean = 31 m; median = 23 m), depending on accessibility and topography of the area, and roughly 3 m in vertical height (from the waterline at low tide to the high intertidal). At each observation site and day, surface water temperature was recorded using a handheld YSI meter (model 85; Yellow Springs, OH), and every sea star within a fixed plot was counted and observed for signs of wasting disease. Sites were grouped into those with surface water temperatures above *versus* below 15 °C at time of sampling. We estimated time to 50% mortality (LT_{50}) for each site by linear interpolation between the immediately preceding and following measurements and compared the two temperature groups using a two-tailed *t* test. In the same time frame, subtidal surveys were performed at seven sites without temperature data. Subtidal belt transects (20 m × 4 m) were sampled with a minimum 20-m separation between transects; the number of subtidal transects per site varied

with site and sea conditions (1–4 transects per dive; mean = 2.1; median = 2; distances between the start and end points of dives, according to boat-based GPS, ranged from 38 to 120 m). The mean number of sea stars per transect of each focal species on that day was calculated per site surveyed.

Additionally, qualitative observation data were collected on a weekly basis in fall 2014 (October to mid-December) as part of a subtidal ecology class at Hopkins Marine Station in Pacific Grove, Monterey, California. At least 16 transects (30 m × 2 m) were completed each sample day at depths of between 8 and 11 m, sampled by two student divers (with half checked by instructors snorkeling [P. Raimondi, M. Carr]). Observations of sea star presence and health were recorded for all species encountered by divers each week, which allowed for documentation of when signs of SSW first emerged within each species and when species were no longer present.

SSW-associated mortality and wave exposure. *Pisaster ochraceus* mortality at sites in north-central California was estimated by quantifying the difference in the densities between 2012–2013 (pre-SSW) and 2014–2015 (after major mortality) (Schiebelhut *et al.*, 2018). Densities were estimated using GPS-tracked 2-m-wide walking transects in each of two areas within a site, often separated by about 100 m on either side of a cove or headland. The percent change in density between time points was reported. Sites spanned three counties: Mendocino (Moat Creek, Iversen Point, Serenisea), Sonoma (Del Mar Landing, Sculpture Point, Fisk Mill Cove, Philips Gulch, Windermere Point, Twin Coves, Bodega Head), and Marin (McClures Beach, Lifeboat House, Palomarin, Duxbury Reef).

Mean significant wave height data at the 15-m isobath were obtained from the Monitoring and Prediction System (MOPs) model provided by the Coastal Data Information Program (O'Reilly *et al.*, 2016). Each of the two areas of a site corresponded to a single MOPs model site, except for Bodega Head, at which the two areas surveyed corresponded to different MOPs model sites and were therefore reported separately. These data are likely overestimates of shoreline wave height, because shoreline survey sites are often sheltered by offshore rock outcrops and headlands, but should be broadly representative of shoreline conditions, barring any modification by small-scale coastal topography. Because these survey sites were broken into two distinct areas, differences in wave exposure were qualitatively assessed between the two areas, using predominant wave direction, expected refraction and sheltering, and 10 years of personal observations working at the sites. Sites were split into two categories: (1) those composed of two areas with different wave exposure, that is, "more" and "less," and (2) those for which the area that received greater wave exposure could not be confidently determined, in which cases the north side of each site was arbitrarily denoted as "area 1" and the south side "area 2." For each of the groups separately, a one-tailed paired *t* test was conducted between each of the areas within a site to assess whether they differed significantly in terms of mortality.

Environment-species integration

A subset of species for which we have estimates of SSW impact was used to explore the relationship between a suite of organismal traits and wasting. Collection of trait data is described in detail in Schiebelhut *et al.* (2022b). Briefly, traits used here include categorically coded traits (developmental mode, diet, and habitat) and continuous traits (minimum depth of occurrence, maximum depth of occurrence, and median month of peak reproductive period). The SSW impact was coded according to the culmination of analyses herein—population size nadir in 2013, direct observation of SSW, likelihood of an extended period of decreased population size post-2013—and its intersection with prior estimates of severity by MARINe (2018). We recognized four categories of impact: 3 = high (multiple lines of evidence of high impact), 2 = medium (multiple lines of evidence of medium effect or some lines indicating high and others low effect), 1 = low (one or more lines of evidence of low effect), and 0 = no evidence of substantial impact. Several species were included for which we did not have SSW impact estimates, so we could explore whether we might expect them to have wasting impacts based on their traits.

We conducted a principal component analysis (PCA) with function "PCA" from FactoMineR (Lê *et al.*, 2008) to assess the strength of the relationship between six variables: developmental mode = (benthic lecithotroph [*i.e.*, brooding]), (pelagic lecithotroph), (pelagic planktotroph), or (mixed benthic and pelagic lecithotroph); depth of deepest occurrence; depth of shallowest occurrence; habitat = (rock), (soft sediments), (rock, gravel, pebbles, cobbles), or (rocks and soft sediments); reproductive season = median month of peak reproductive period; and diet. Principal axes were generated to explain the maximal amount of variance in the data. The PCA algorithm generates principal components (axes) where the data show the maximum amount of variance (Legendre and Legendre, 2012). The PCA outputs a two-dimensional ordination plot that visualizes the relationships between predictor variables. Missing data and data normalization were addressed using the "pca.mvreplace" function of mdatools R package (Kucheryavskiy, 2020). A scree plot test was used to identify the two significant axes in the PCA, and the PCA was visualized using the R functions "fviz_eig" and "fviz_pca_var" of the factoextra R package, respectively (Kassambara and Mundt, 2020).

Results

Broadscale analyses

Environment. The SST (Fig. 1b, c) exhibits typical trends across latitudes and seasons. Distinct spatial features that

overlay the latitudinal trend in seasonal climatology (Fig. 1c) include warmer water in bays (*e.g.*, San Francisco Bay, cell 31) and gulfs (*e.g.*, Southern California Bight, cells 18–23) in summer and cooler waters associated with upwelling maxima at headlands (*e.g.*, Cape Arago, Cape Mendocino, cells 35, 42). Seasonal trends shift from British Columbia and Alaska, where the coolest months are February/March/April, to strong-upwelling regions like Oregon and north/central California, where the coolest months are April/May/June. The warmest months are generally August toward the north and September toward the south. Latitude-dependent interannual cooling and warming overlay these seasonal patterns (Fig. 1b). Although 2011 and 2012 exhibited cool anomalies in general, distinct brief warm anomalies of ≥2 °C occurred off Baja California in September–October 2012 and off Oregon and Washington in September 2013. These were followed by a few years of widespread and persistent positive anomalies (2014–2016) associated with the Pacific "warm blob" and developing El Niño conditions, most notable in winter (September/October–February/March 2014 and 2015) and at lower latitudes from Baja California to Washington. The strongest warm anomalies in Alaska occurred in the summer of 2016. While cooler conditions prevailed throughout the study region in 2017 and 2018, warm anomalies returned in 2019, particularly in Alaska and also in fall in Oregon and Washington. Within bays, anomalies were often inconsistent with open coastal waters; for example, San Francisco Bay exhibited marked positive anomalies 2017–2020, while open waters in central California were mostly cooler than average.

Surface Chl *a* concentration exhibits a seasonal cycle, peaking in late spring or early summer at most latitudes (Fig. 1e). More persistent Chl *a* levels are observed in bays downstream of upwelling centers, for example, just north of Bahia Magdalena (cells 2–3), Guerrero Negro (9–11), Southern California Bight (21–23), Gulf of Farallones (29–32), just north of Cape Mendocino (38–39), and just north of Cape Arago (42–43). More persistently high Chl *a* also occurs in the Salish Sea and other inland waters off British Columbia and southeast Alaska. The Chl *a* anomalies are at smaller local scales than SST (Fig. 1d). The only persistent anomaly is off British Columbia and Washington in early 2015.

Upwelling winds are most intense off north-central California, where they persist year-round with a peak in April–June (Fig. 1g). Off Baja California and southern California, upwelling winds are weaker and peak earlier. North of Cape Mendocino in northern California, the upwelling season alternates with a winter downwelling season, and off Alaska, wind in the summer months is neither upwelling nor downwelling favorable. Positive anomalies (stronger than usual upwelling winds) occurred off Baja California during 2011 and 2012, off California in summer 2012 and spring 2013, and in the 2013–2014 winter from San Francisco north to Alaska (Fig. 1f). By contrast, the winters of 2015–2016 and 2016–2017 are marked by strong downwelling (negative anomalies) from Oregon to Alaska and by weaker upwelling off northern/central California.

Wave height exhibits strong seasonality (*i.e.*, bigger waves in winter) and a strong correlation with latitude (*i.e.*, bigger waves at higher latitudes [when considering outercoast sites]; Fig. 2a). Overall, winters at the start of 2013–2015 exhibited lower wave heights than other winters, and the largest wave heights were observed in the 2015–2016 winter throughout the northeastern Pacific study region.

River discharge, a proxy for freshwater exposure and allochthonous materials of terrestrial origin, shows considerable variation, with dry and wet years in quick succession. Considerable local variation is indicated by variation among watersheds in a given state, but peak discharge events are concurrent from northern California to Washington (*e.g.*, peaks in late 2013 and late 2016 into 2017; Fig. 2b). Peak freshwater runoff in Alaska in 2014 and 2015 coincided with dry or normal years to the south, whereas 2017 was a wet year in Oregon and California but a dry year in Alaska. In general, drier-than-usual conditions were observed in California at the time of the SSW outbreak in 2013–2014. However, wetter-than-usual conditions were observed in Alaska at the time of the inferred SSW outbreak in 2015–2016.

Biology. The patterns of abundance of sea stars in the northeastern Pacific intertidal and subtidal zones vary greatly by species and through time (Fig. 3). Minimal and maximal abundances occur in at least one species in every time period considered, that is, pre-2013 and annually since (Fig. 3a). Considering all 65 species and all years for which we had data, maxima predominate in pre-2013 (17 species), while minima predominate in 2013 (26 species) and 2019 (36 species; Fig. 3c). Minima were slightly more intense in intertidal/shallow subtidal species (9 of 12 species; 75%) than in deeper-water species (19 of 52; 37%) in 2013. While mean relative abundance increased consistently from 2013 to 2018, the mean annual relative abundance remained lower in all post-2012 years than in pre-2013. While this could be a function of comparing 12 years pre-2013 with only 8 years post-2012, the long-term average in both periods would be expected to be the same if population sizes overall were stable or fluctuated randomly around a mean, and this clearly did not occur. Moreover, mean relative abundance appears to have declined a second time in 2019.

For species for which only presence and/or absence data exist, species showed great variability in temporal patterns of occurrence (Fig. 3b). While overall, species were frequently absent in one or more years post-2012, there may be little information in contrasting a presence during the years pre-2013 with an absence in one or more years post-2012, particularly for small and cryptic species in the genera *Henricia* and *Leptasterias*.

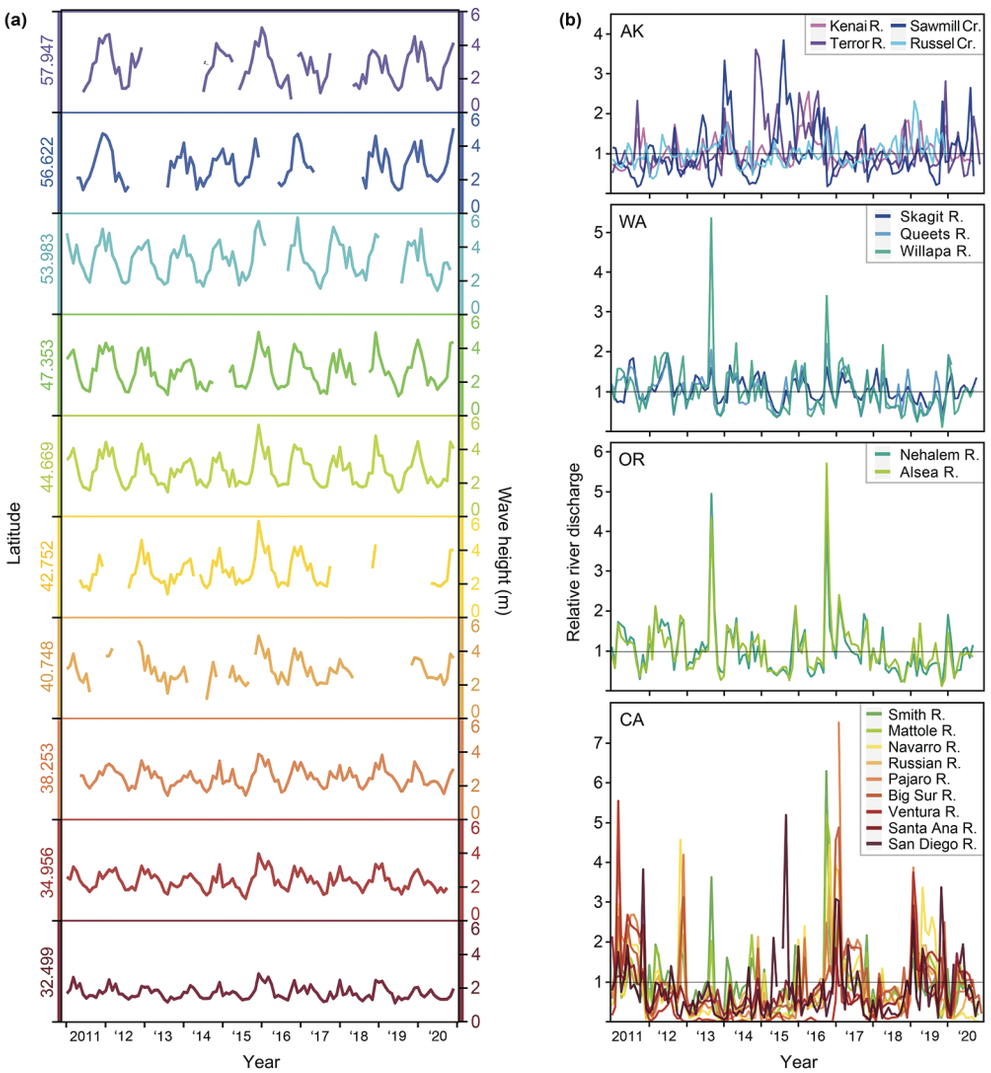

Figure 2. Large-scale spatial and temporal variation in wave exposure and freshwater influence for 2011–2020. (a) Wave height variation at stations from southern California to southeastern Alaska, showing greater wave exposure at outercoast buoys and more marked seasonality in more northerly regions. (b) Relative river discharge for drainages grouped by state to show regional concurrence and variation in precipitation and freshwater influence. The horizontal line at $y = 1$ represents the long-term average; note that the greater amplitude in relative discharge indicates greater episodic variation in more southerly regions, although absolute volumes are less.

Data on the prevalence of SSW are available for 12 intertidal/shallow subtidal species, mostly beginning in 2014. The greatest taxonomic and latitudinal breadths of SSW occur in 2014, though with a notable secondary peak in 2016 in the northernmost cells and species (Fig. 4). The prevalence of wasting declined substantially within 1–2 years after the peak in most species, though SSW-like symptoms have remained present at low prevalence rates in most species and latitudes.

Data on recruitment are available for only eight taxa (Fig. 5). For half of these, we infer that recruitment has been nonzero in all surveyed years post-2013. Data for 2013 were available only for *Pisaster ochraceus* and were also nonzero. Information on latitudinal patterns in recruitment are informed primarily by data on *P. ochraceus* recruitment, which intensified in 2015. Recruitment south of Point Conception (southern California) has been notably weak to absent and waned in recent years but remained strong in northern California and Oregon. Farther north, recruitment appears to have occurred in most years, but not in high numbers.

Small-scale analyses

Time line of SSW progression. Three analyses of SSW in the wild, one intertidal and two subtidal, emphasize the rapidity with which SSW can cause substantial population declines once symptoms first emerge. The 2014 intertidal study of *P. ochraceus* in the San Juan Islands, Washington, showed that populations can proceed from almost 100% asymptomatic individuals to over 80% symptomatic

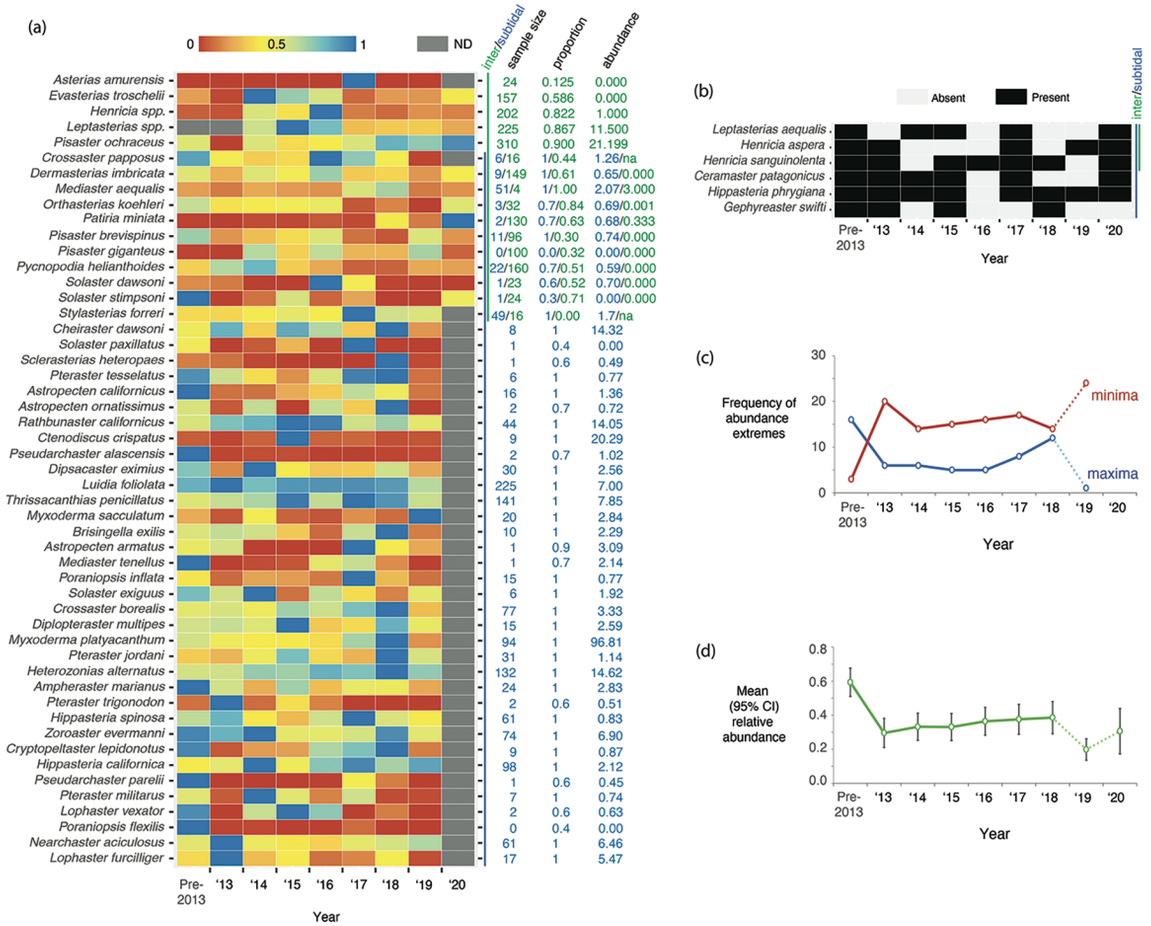

Figure 3. Abundance and presence/absence dynamics of northeastern Pacific sea stars from 2000 to 2020. (a) Relative abundance of 51 regularly encountered asteroid species through time. The heatmap is standardized to emphasize the intraspecific dynamics of each species, rather than the relative abundances of different species, by dividing all annual abundances of a species by that species' maximum abundance. The maximum observed abundance of any species is therefore 1.00 (dark blue); if two or more datasets were available for a species, abundances were averaged after standardization, in which case the maximum abundance may be <1.00. Thus, some taxa may be far more abundant than others, which is represented by the three numbers at the end of each row: sample size (the number of positive surveys [green, intertidal transects; blue, trawls]), proportion (of transects that were nonzero or of trawl years in which the 25th percentile was greater than zero), and abundance (median for transects, median of the annual medians for trawls). Dark gray cells indicate no data (ND) for that species in that year; the majority of missing data are for species surveyed only by the National Marine Fisheries Service, which did not conduct surveys in 2020 because of COVID-19 restrictions. Species with data in 2020 were present in intertidal surveys. (b) Occurrence of species for which abundance data were not available. In both (a) and (b) taxa are ordered by relative rank of their depth distribution, from the shallowest (top) to the deepest (bottom), based first on whether they occur intertidally, then second on the median depth of species occurrence, and third alphabetically. Note that in this figure redder colors represent low abundance, that is, ostensibly "worse" years for sea stars. (c) Frequency of minimal and maximal abundances of 65 sea star species through time, that is, the 51 species in (a) plus 14 others recovered less regularly. Dotted lines connecting the datum for 2019 indicate an effect coincident with a marine heatwave but possibly exacerbated by undersampling of rare species due to a reduced number of trawls. (d) Mean relative abundance of northeastern Pacific sea stars (±95% confidence intervals [CIs]) had a nadir in 2013 and may have ratcheted down further in 2019. Dotted lines connecting the datum for 2019 indicate an effect possibly exacerbated by undersampling of rare species due to a reduced number of trawls.

individuals within 3 weeks, irrespective of water temperature, though cooler temperature is associated with later onset (mean ± SD LT_{50} = 67 ± 10.0 *vs.* 45 ± 7.8 days; P = 0.009) and a slight lengthening of the duration (Fig. 6a). Likewise, a multispecies study off Pacific Grove, California, showed that wasting may be equally rapid in subtidal populations, although the rate of extirpation of sea stars from a locality is dependent upon species (Fig. 6b), a pattern also apparent in subtidal populations in the San Juan Islands (Fig. 6c). These multispecies studies showed differences in response times associated with different local environmental conditions and taxa and illustrate how the impacts of SSW become temporally drawn out when assessed at the community level.

SSW-associated mortality and wave exposure. Pisaster ochraceus at central California sites with low wave height (*e.g.*, <0.7 m) experienced high (>80%) mortality; however, at sites with greater wave exposure, there was high variability in mortality (Fig. 7a). Within-site comparisons of areas with either different or undifferentiable qualitative

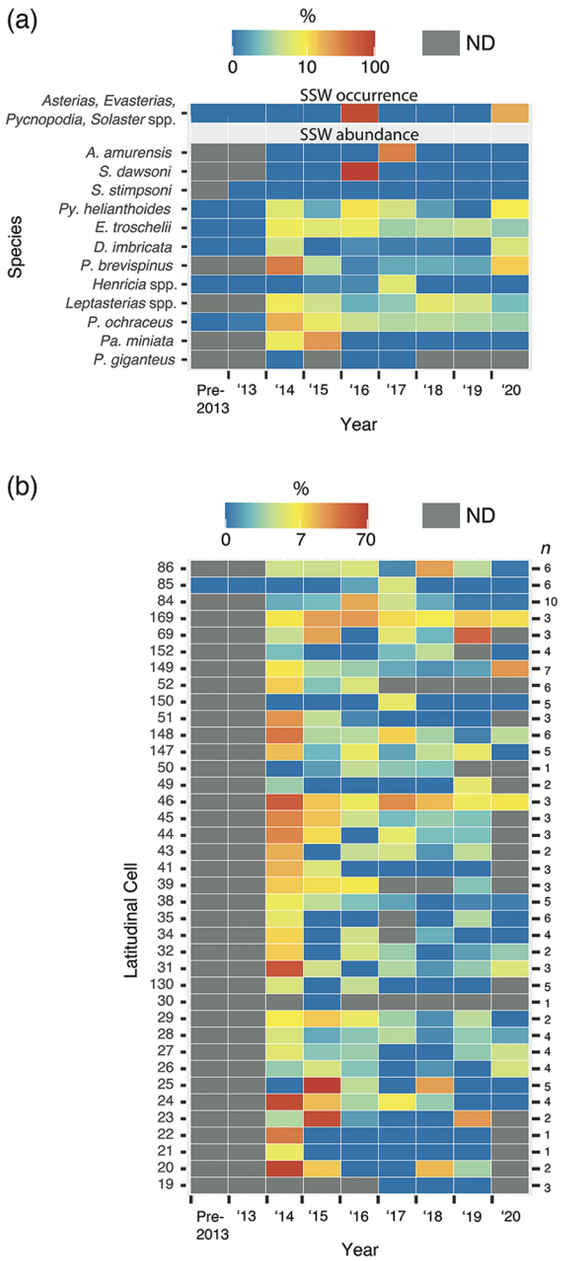

Figure 4. Sea star wasting (SSW) impact by taxon and by latitude. (a) Prevalence of symptomatic individuals in taxa for which data were collected. The top panel shows the prevalence across five species for which only presence/absence of SSW was recorded; these are primarily data from Alaska. The bottom panel shows the prevalence within each of 12 species for which percent prevalence was quantified. The species are organized by mean latitude of cells in which measurements were taken for that species, with more northerly distributed taxa toward the top of the panel and more southerly distributed taxa toward the bottom. All taxa are shallow-water taxa; SSW was not recorded for deeper-water taxa in the National Marine Fisheries Service trawl surveys. (b) Community-level SSW prevalence, in about half-degree cells, ordered by latitude from northwest (top) to south (bottom); cell numbers to the left of the panel show the latitudinal cells; two-digit numbers correspond to outercoast sites; and three-digit cells indicate inshore divisions around San Francisco, Puget Sound and Vancouver Island, and southeastern Alaska. Numbers to the right of the panel show the number of species for which data were included in each latitudinal cell. Note that in this figure redder colors represent high disease prevalence, that is, ostensibly "worse" years for sea stars. In both panels, dark gray cells indicate no data. Genus abbreviations are as follows: *A.*, *Asterias*; *D.*, *Dermasterias*; *E.*, *Evasterias*; *P.*, *Pisaster*; *Pa.*, *Patiria*; *Py.*, *Pycnopodia*; *S.*, *Solaster*. ND, no data.

wave exposures showed increased mortality with decreased wave exposure ($t = -3.85$, df $= 5$, $P = 0.0060$; Fig. 7b) and no significant difference in mortality between similarly exposed areas ($t = -0.73$, df $= 3$, $P = 0.2596$; Fig. 7c).

Environment-species integration

The first three principal components (PCs) explain 77.7% of variation (axis 1: 37.5%; axis 2: 24.8%; axis 3: 15.4%) in the distributional, habitat, and dietary characteristics of northeastern Pacific sea stars (Fig. 8). The PCA did not clearly differentiate sea stars that exhibited low-, intermediate-, or high-severity SSW, indicating that there was no clear relationship between wasting and any single characteristic or suite of characteristics included. The close grouping of congeneric species (*e.g.*, *Asterias* spp., *Pisaster* spp.), for example, indicates ecological similarity, though inferred SSW impacts were sometimes quite different. However, the first axis illustrates a tendency for species exhibiting high and some mortality to occur farther to the left (*i.e.*, shallower) than the remaining ones. Thus, minimum and maximum depth and early reproductive season were the strongest contributors to the first principal component (PC1). Notably, one of the two species in this analysis that experienced no substantial SSW impact, *Rathbunaster californicus*, is a deeper-water species and is segregated strongly along this axis from its sister taxon, *Pycnopodia helianthoides*, which is found in shallower water and was among the most negatively affected by SSW. The other species in this analysis that experienced no substantial SSW impact, *Ceramaster patagonicus*, is also a deeper-water species that segregates with species with low severity of SSW (Fig. 8) toward the right of PC1. For species with unknown SSW impact, positioning in the PCA would implicate *Asterias forbesi*, *Asterias rubens*, *Heliaster kubiniji*, and *Henricia pumila* as being medium to highly susceptible to SSW, while *Leptychaster pacificus* would have relatively low susceptibility to SSW. The presentation and mechanisms of these spatially and temporally distinct events, which have all been referred to as "SSW" in the literature, are of course debated as to whether they represent the same phenomenon (Oulhen *et al.*, 2022).

Discussion

Broadscale analyses

Biology. Our narrative analysis of 65 sea star species, across geographic scales from single-site to coast-wide and temporal scales from weeks to decades, shows that the first signs of SSW appeared in 2013, were widespread by 2014,

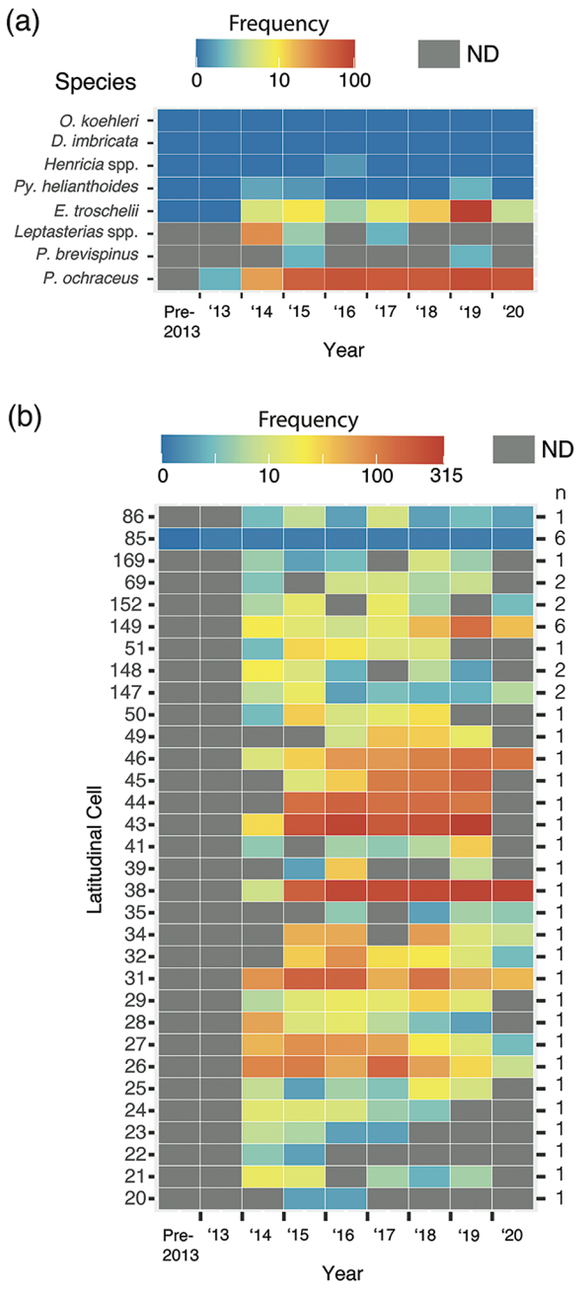

Figure 5. Sea star recruitment by taxon and by latitude. (a) Number of recruits per 200 m^2 for the subset of species for which data were collected, organized by taxon. All taxa are intertidal/shallow subtidal; sea star wasting (SSW) was not recorded for deeper taxa. The species are organized by mean latitude of cells in which measurements were taken; that is, more northerly distributed taxa are toward the top of the graph, and more southerly taxa are toward the bottom. (b) The same data reorganized by latitudinal cell, with two-digit numbers to the left of the panel corresponding to outercoast sites and three-digit cells indicating inshore divisions around San Francisco, Puget Sound and Vancouver Island, and southeastern Alaska. Numbers immediately to the right of the panel show the number of species contributing data to that cell. Mostly there is one species per cell, that is, *Pisaster ochraceus* (cells 20–50, 51) or *Evasterias troschelii* (cells 169, 86), or two species (*i.e.*, *P. ochraceus* and *E. troschelii*; cells 147, 148, 152, 69), with surveys of other species contributing to a small number of cells (149 = *E. troschelii*, *Henricia*, *Leptasterias*, *Pisaster brevispinus*, *P. ochraceus*, *Pycnopodia helianthoides*; 85 = *Dermasterias imbricata*, *E. troschelii*, *Henricia*, *Orthasterias koehleri*, *P. ochraceus*, *P. helianthoides*). Note that because surveys occupy a tiny fraction of each cell and habitat is heterogeneously distributed, these numbers should not be extrapolated to estimate total counts. Note also that in this figure redder colors represent higher numbers of recruits, that is, ostensibly "better" years for sea stars. In both panels, dark gray cells indicate no data. Genus abbreviations are as follows: *D.*, *Dermasterias*; *E.*, *Evasterias*; *O.*, *Orthasterias*; *P.*, *Pisaster*; *Py.*, *Pycnopodia*. ND, no data.

and continued to expand northward in 2015 and 2016 (Menge *et al.*, 2016; Miner *et al.*, 2018; Konar *et al.*, 2019). These dynamics are implied in dramatic declines in abundance across many species—nadirs were measured in 26 species in 2013—though the first direct quantitative estimates of the incidence of SSW are from 2014, when a suite of studies began assessing the proportion of sea stars displaying symptoms. Sea star wasting impacted different species at different times and in different places with varying intensities, and it has continued to be observed since, though at a lower frequency.

The novelty and impact of our analysis is sixfold. One, it points to an effect concentrated in intertidal/shallow subtidal communities. Considering species for which there are pre-2013, 2013, and 2014 data, abundance minima in 2013 prevail in 75% of intertidal/shallow subtidal species (9 of 12) but are half as frequent (19 of 52; 37%) in deeper-water species. Because intertidal and subtidal populations of a given species show somewhat similar dynamics despite differences in methods, locations, and timing of surveys (Supplementary Document 4), the difference in SSW impacts between intertidal/shallow subtidal and deeper subtidal communities is best interpreted as being a consequence of different species composition or different distribution (habitat or depth) of those communities and their attributes.

Two, our analyses reveal that deepwater communities also experienced a nadir in 2013. The absence of a direct assessment of SSW means that we cannot know whether deepwater species were affected by SSW or whether declines in abundance were indirect consequences of (tele)connections between surface oceanographic events and deepwater, but it does indicate that dynamics of deepwater species and communities are in part tied to surface events, perhaps through allochthonous inputs of dead or living matter. The NMFS trawl data also show that some deepwater species have lowest abundances at other times, likely for other reasons, so these allochthonous processes can be influential but are unlikely to be omnipotent. One of the most intriguing patterns in the data, however, is an apparent second dramatic decline in abundances of multiple species in 2019. This drop coincides with the resurgence of a "warm blob" (Cornwall, 2019; Suryan *et al.*, 2021) but is not marked by increased prevalence of SSW. The observation is challenging to interpret due to there being fewer trawls in 2019,

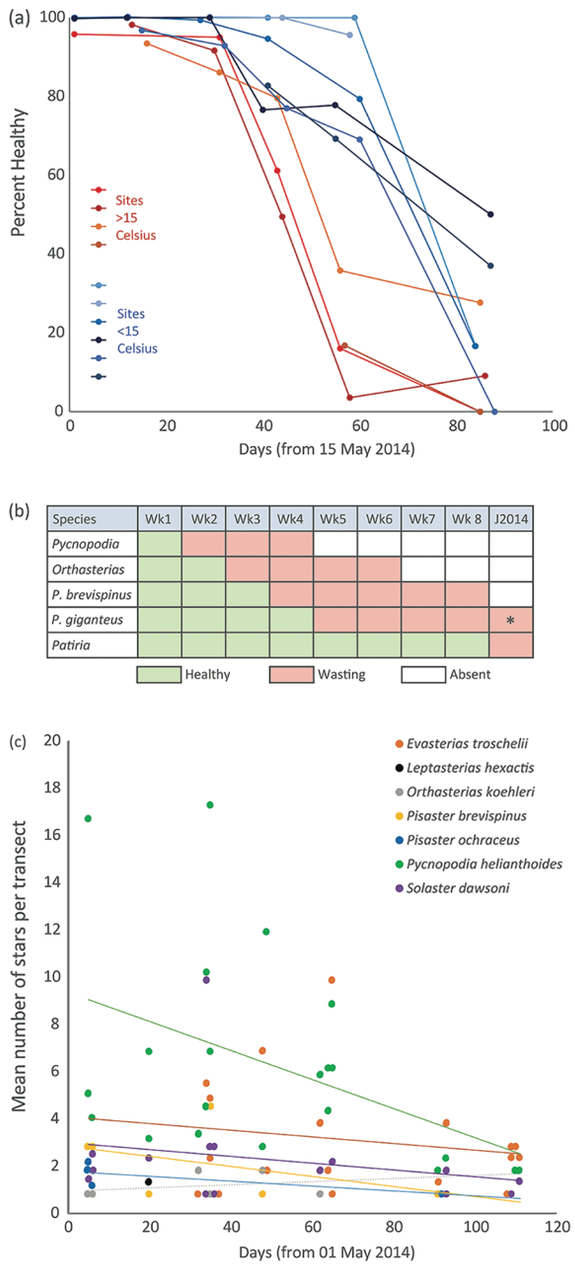

Figure 6. Three fine-scale perspectives on the rates of onset and progression of sea star wasting (SSW) in the wild. (a) *Pisaster ochraceus* in the intertidal zone of the San Juan Islands, Washington, in 2014, with fixed plots (mean = 2.4 [median = 3] per site, of mean length 31 m [median = 23 m]) in different locations shown by different lines and segregated by color: red, sites with sea surface temperature >15 °C; blue, sites with sea surface temperature <15 °C. (b) Subtidal sites at Monterey, California, between October and December 2014. The asterisk indicates that *Pisaster giganteus* was exceptionally rare during this period, leading to very small sample size. (c) Sea star community data, by species, from belt transects (mean = 2.1; median = 2 per site) in the subtidal zone of the San Juan islands, excluding *Henricia*, which showed little SSW response at the time.

which could lead to fewer observations of rare species; however, the drop also occurs in some common species and is robust to calculating population dynamics in several different ways (Supplementary Document 5), suggesting that it was a real phenomenon.

Three, our datasets give a quantitative estimate of the taxonomic extent of SSW. Considering the most direct evidence—observation of wasting—10 species that occur in the intertidal zone exhibited SSW symptoms (Fig. 4a). Considering additional indirect evidence, we may infer that up to 19 additional species with subtidal populations that showed reduced populations in 2013 relative to 2012 and 2014 may have been impacted during the mid-2010s outbreak (Fig. 3). Of these, only five—*Cryptopeltaster lepidonotus*, *Pisaster brevispinus* (also intertidal), *Pseudarchaster alascensis*, *Pycnopodia helianthoides* (also intertidal), and *Zoroaster evermanni*—showed the persistently reduced abundances (Supplementary Document 6) typical of species in intertidal surveys known to have experienced substantial mortality from SSW. The 14–29 unique species thus implicated include all five "high mortality," 5–6 of 8 "some mortality," and up to 2 of 10 "likely affected, mortality level not well documented" species listed by MARINe (2018). Though there may be some ascertainment bias introduced by comparing across datasets that overlap only partially, there appears to be clear and consistent evidence of substantial SSW outbreak-related impacts in a little over one dozen species, whereas impacts in other taxa may be indistinguishable from background levels of wasting or other causes of mortality.

Four, we have improved estimates of the prevalence of SSW in affected species during the outbreak and how it varied among species and through time. For example, *P. brevispinus* and *Pisaster ochraceus* suffered higher prevalence (maximum = 35%, 19%, respectively) and *Dermasterias imbricata* lower prevalence (maximum = 5%). The highest prevalences (100% in *Solaster dawsoni*), however, were recorded in 2015–2016 as SSW was surging in more northerly studies. Even though the *S. dawsoni* estimate is from a relatively small sample size, it suggests that the most intense mortalities in southern species may have passed unmeasured due to a dearth of studies in 2013. This interpretation is supported by data on *P. helianthoides*, for which the maximum prevalence reported here is only 5%–10% (peaking in 2016 with Alaskan datasets), though it is widely reported to have suffered the greatest losses and to have been extirpated from California and Oregon. We also are able to make a rough approximation of background levels of SSW-like symptoms, which is present chronically during nonoutbreak periods (Eckert *et al.*, 2000). Considering all species that exhibited SSW in one or more years (Fig. 4a), and excluding the single highest observed annual prevalence for each species (*i.e.*, the most obvious outbreak years), gives an upper estimate of the chronic mean prevalence of SSW as 1.7%, which compares well with the estimate of 2% by Eckert *et al.* (2000).

Five, a majority (6 of 8) of studied intertidal/shallow subtidal species recruited juveniles shortly after the acute

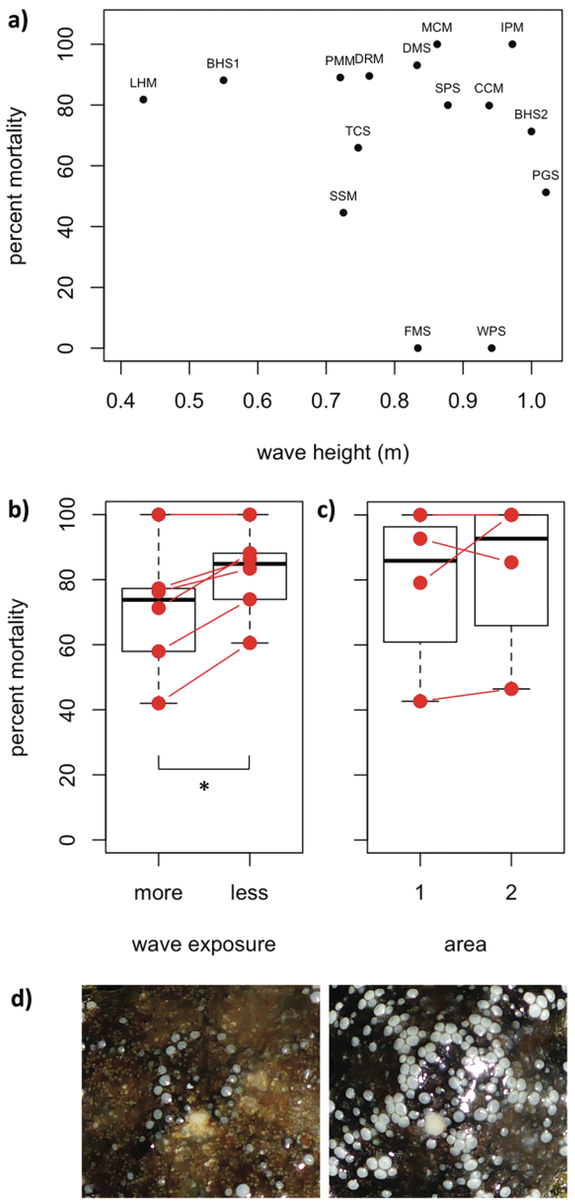

Figure 7. Fine-scale relationships between wave exposure and mortality in *Pisaster ochraceus*. (a) Mean significant wave height *versus* mean mortality by site. Site abbreviations are as follows: BHS, Bodega Head; CCM, McClures Beach; DMS, Del Mar Landing; DRM, Duxbury Reef; FMS, Fisk Mill Cove; IPM, Iversen Point; LHM, Lifeboat House; MCM, Moat Creek; PGS, Philips Gulch; PMM, Palomarin; SSM, Serenisea; SPS, Sculpture Point; TCS, Twin Coves; WPS, Windermere Point. (b) Comparisons of within-site differences in wave exposure between each of the two areas; areas with lower wave exposure had higher mortality ($P = 0.0060$). (c) Comparisons of areas for which we could not confidently determine which area received greater wave exposure (so we assigned the north side of each site as area 1 and the south side as area 2); areas were not significantly different ($P = 0.2496$). (d) An example of the differences in tubercle (white knobby structure) densities in *Pisaster ochraceus* shown for the same area of disk.

outbreak, and while not captured by our data, observations of juvenile *D. imbricata* were made by MARINe researchers in California and Washington (CMM, pers. comm.). For at least half of the species, recruitment immediately followed the die-off, and the number of recruits varied greatly by species, year, and latitude. Yet based on the criteria used, we infer that many of the studied species continued to recruit in most subsequent years included in this study, though recruitment success was spatially heterogeneous (*e.g.*, central *vs.* southern California) and in places has waned through time. We extrapolate that other species also recruited consistently because the overall relative abundance of sea star communities increased post-2013. Better understanding of the geographic and parental sources of recruits, and species' ecologies more generally, is essential for developing a conceptual framework for recovery rates and for better predicting the resilience of sea star populations to future SSW outbreaks (Schiebelhut *et al.*, 2018, 2022a).

Six, it is possible to estimate the duration of the epidemic at 2–3 years, based on when it started at particular latitudes and inferred end dates based on the preceding information. Considering southern latitudes, for example, diseased sea stars were first noted in central and southern California by fall 2013 (Miner *et al.*, 2018) and increased rapidly—affecting first *P. helianthoides* then *P. ochraceus* (19% prevalence) and later *Patiria miniata* (25% prevalence)—but by 2016 the prevalence of SSW among these and other species in southerly communities had dropped to ~2.5% overall (Fig. 4b, cells ca. 20–34). In areas where the disease peaked later, for example, in Alaska in 2015–2016, SSW prevalence again subsided to ≤2% by 2018 (Fig. 4b, cells ca. 69–86). Though individual species may have experienced more short-lived effects, different species' tolerances led to persistence of symptoms at elevated rates within and among communities for ~3 years. Furthermore, the repercussions have lasted much longer. Although recruitment began largely immediately for many species and places (albeit heterogeneous and with notable exceptions such as *P. helianthoides* in California), the overall mean relative abundance of sea star communities has responded only slowly. Of particular concern is the indication that mass-mortality events may occur at shorter periodicities than the duration of recovery, potentially ratcheting populations toward extirpation, communities toward collapse, and species toward extinction.

Environment. It is generally suspected that one or more environmental factors contributed to the onset of, or exacerbated, the epidemic, whether or not an infectious pathogen is associated with SSW. The environmental factor(s) may be acute (*e.g.*, a marine heatwave event), chronic (*e.g.*, a climate change trend), or both. They may act in concert and/or sequentially. As such, environmental factors bear examination as potential causes, facilitators, or stressors. If associated with SSW, there should be an equally clear contemporaneous signal in the environmental data. In this context, distinct patterns and strengths of anomalies in the environmental variables we considered are notable candidates for further exploration.

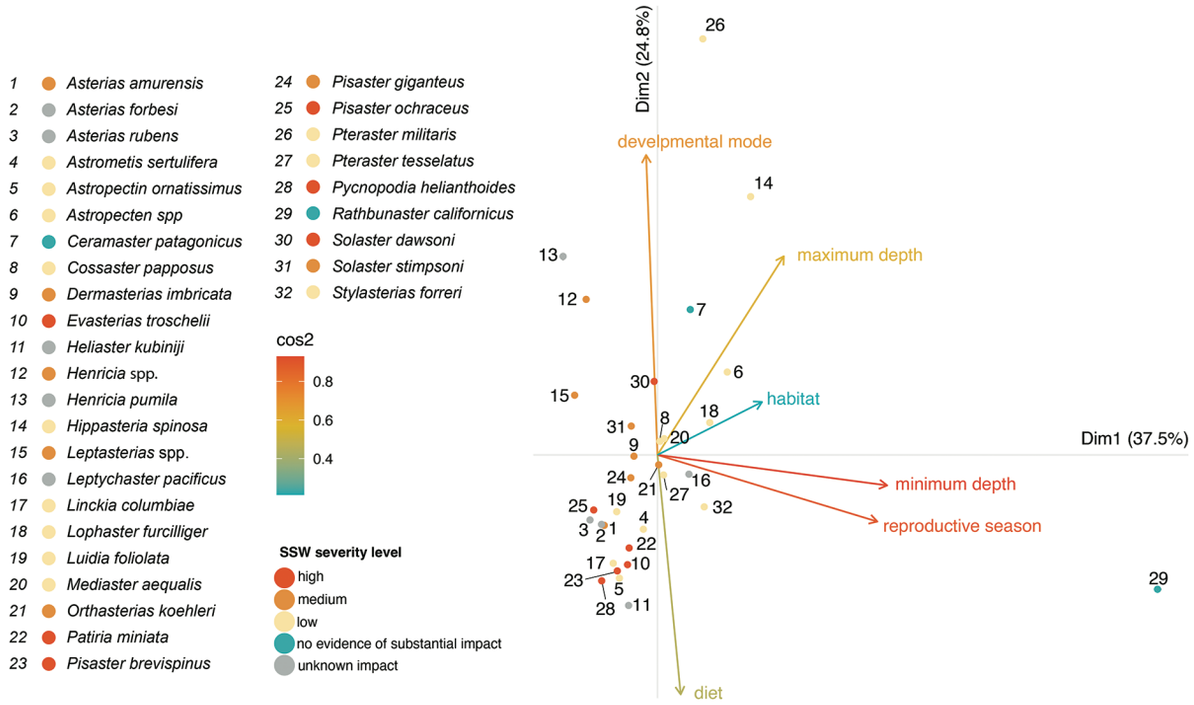

Figure 8. Principal component analysis summarizing ecological similarity among sea star species, color-coded with the added context of species' susceptibility to sea star wasting (SSW) as estimated in this study. Each point in the plot represents a distinct species; their proximity indicates their relative ecological similarity. *Asterias forbesi* and *Asterias rubens* are Atlantic species included for comparison. No data exist for SSW impacts on species in gray, which are included here to explore whether predictions may be made about SSW susceptibility based on ecological characteristics. Note, however, that the general term "sea star wasting" used globally for wasting events could indeed have different, as yet unknown, causative agents. The vectors depict the loadings of each variable on the two principal dimensions, with angles between vectors indicating their correlations; direction and length of vectors reflect the direction and strength of the influence of the variables: developmental mode, maximum depth (depth of deepest occurrence), minimum depth (depth of shallowest occurrence), habitat (substrate type), reproductive season (median month of peak reproductive period), diet (primary prey type or foodstuff). The color of each vector indicates that variable's coefficient of similarity (cos).

For example, Chl *a* concentration appears largely non-anomalous spatially and temporally throughout the region considered, although small-scale anomalies do occur, specifically in bays and inland waters that are highly variable from month to month. By contrast, mean SST and BUI have clear and strong anomalies that first appeared in 2013, though their spatial and temporal development differ. The SST 1–3-month warm anomaly begins in the south in early to mid-2013 and expands northward through British Columbia by September 2013 before dissipating. It returns much more expansively and persistently in 2014 and 2015, again with the strongest anomalies progressing from south to north, this time into Alaska over a period of 6–8 months. This strong and widespread anomaly subsided by 2017 but reprised in more limited form in 2019, concentrated on Oregon, Washington, and Alaska, associated with the return of the "warm blob" (Cornwall, 2019; Suryan *et al.*, 2021); on the other hand, BUI tends to show a distinct spatial difference between southern/central California and northern California, with strongest anomalies in the latter. The strongest positive anomalies (strong upwelling) occurred in early 2013 and again in the 2013–2014 winter, extending from central California to Alaska, and briefly reprised in Alaska in November 2014 and November 2015, but 2016 saw anomalously low BUI across the entire northern region. The remaining two variables we considered—wave height and river discharge—are more variable and spatially more patchy, making interpretation of broad patterns more challenging. Nonetheless, wave energy appears to be consistently low in the winters at the start of 2014 and 2015 as SSW emerged and spread and higher in winter 2015–2016 as SSW dissipated. River discharges are spatially highly variable but appear unusually and consistently low in California (particularly southern California) through 2013–2014 (except for one month in late 2013), though this signal weakens as one moves into northern California and more so even farther northward, with 2015–2016 tending to be higher than average discharge in Alaska.

What may we infer about cause and effect, then, from environmental data? The biological patterns predominantly show (i) onset and most intense mortality in 2013 in intertidal/shallow subtidal species, (ii) still high rates of prevalence of SSW in 2014 from California to Washington and in 2015–2016 in Alaska, and (iii) subsidence 2–3 years post-outbreak. Of the environmental factors considered, the most consistent match is with elevated SST, which has

corresponding spatial and temporal patterns. The warm anomaly in 2013—coming atop seasonal warming and a half-century trend of global change (Rasmussen *et al.*, 2020; Frankson *et al.*, 2022)—may have influenced SSW directly, though the strongest SST anomalies may lag SSW, suggesting that onset and persistence could involve different or indirectly associated mechanisms possibly in novel combinations. Chlorophyll *a* seems to neither be consistent enough nor have sufficiently strong temporal or spatial anomalies closely associated with SSW, and BUI appears to have too strong a spatial divide—and too strong a spatial synchrony in the northern region—to be consistently related with SSW coastwide and through time. By contrast, wave exposure and river discharge are intriguing because extremes of each occur in both California and Alaska in years with elevated SSW, although the extremes differ: being low in 2013–2014 in California and high in 2015–2016 in Alaska. Yet it is possible to imagine these outliers working in complementary ways near the surface. For example, low river discharge and wave height may have facilitated near-surface heating and temperature stratification, leading to highly unusual surface conditions in 2013–2014 in the south. By contrast, increased river discharge in the north may have caused increased freshwater stress at the surface in 2015–2016. Both would be consistent with a more substantial impact on intertidal/shallow subtidal than deeper-water species. Moreover, freshwater runoff and wave exposure are already known to shape sea star communities (Konar *et al.*, 2019) and to have been linked with SSW-associated mortality or survivorship (Dungan *et al.*, 1982; Bates *et al.*, 2009; Konar *et al.*, 2019).

While environmental effects remain unclear, an epidemiological perspective suggests that there are likely multiple ways in which environmental conditions could influence disease transmission and pathogenicity in sea stars. Spatial and temporal heterogeneity in currents, potential pathogens, abiotic environments, and hosts yield complex interactions among potential factors. Thus, the environmental stress that enables an outbreak may not be consistent across the domain, and the environmental influence may be multiphased: for example, (i) dispersion of high levels of pathogen into the region and (ii) environmental stress that allows an outbreak of disease that results in observed mortality. Factors may feedback on themselves (*e.g.*, pathogen evolution), and environmental stress may also be important in persistence of the disease and its impacts.

Small-scale analyses

Establishing a link between the broadscale abiotic and biotic patterns requires additional steps, including smaller-scale analyses that can couple factors more closely both spatially and temporally and experiments that can measure responses to specific manipulations. Experiments gain in precision what they lose in complexity and scope, so here we strike a middle ground by employing several small-scale analyses as convenient intermediates that further explore relationships between temperature and wasting, subtidal-intertidal dynamics in conspecifics, the time line of SSW progression, and association between wave exposure and SSW.

Time line of SSW progression in intertidal and subtidal sea stars in relation to temperature. High-temporal-resolution studies confirmed that the onset of SSW could be rapid and the fatality rate high but variable among species. An association between elevated SST and increased risk from SSW is indicated by high temporal resolution monitoring in the Salish Sea, Washington (Fig. 6a), which showed that the decline in intertidal asteroid population health was more rapidly apparent at sites exhibiting warm temperature anomalies (*e.g.*, Eisenlord *et al.*, 2016). The fortnightly surveys showed that population decline and local extirpation happened on the timescale of weeks, rather than months, indicating that many events could be missed if not regularly monitored. Similarly rapid declines were observed between subsequent spring tide series from early August to late September in Kachemak Bay, Alaska (KAG, pers. obs.). High-frequency subtidal data from the central California coast (Fig. 6b) show similarly rapid declines of individual species but also reveal how variation in the onset and progression of SSW across dominant species—presumably indicating interactions between species' traits, environment, and other factors driving this disease (Schiebelhut *et al.*, 2022b)—ultimately protract the epizootic epidemic (Fig. 6b, c).

Wave exposure (or shelter) and SSW. Microenvironment may also exacerbate or draw out population and community responses. During intensive surveys in north-central California, an absence of sites with both low wave height and low SSW suggested that lower wave intensity (and thus low turbulence and/or small-scale flow) may have contributed to increased *P. ochraceus* mortality (Fig. 7a). Paired analyses contrasting more *versus* less wave-exposed areas within sites controlled for some site-specific heterogeneity and emphasized a possible relationship between wave exposure and vulnerability to SSW (Fig. 7b, c). Although a specific mechanism is unclear, limited flow could lead to the establishment of a microenvironment (*e.g.*, Fifer *et al.*, 2021) that promotes the development of a dysoxia-driven microbial dysbiosis on submillimeter scales on the sea star surface, limiting gas exchange needed for effective respiration at the animal-sea interface and resulting in wasting (Aquino *et al.*, 2021; see also Pespeni and Lloyd, 2023). *Pisaster ochraceus* is known to respond phenotypically to different wave exposures by elongating their shape and increasing the density of tubercles (the hard knobby ossicles protruding from their epidermis; Fig. 7d) with greater wave intensities (Hayne and Palmer, 2013). It remains to be explored whether *P. ochraceus* ecotypes associated with wave-exposed shores (*i.e.*, high density of external hard parts [tubercles]) fared better than ecotypes possessing a greater

surface area of softer external parts. We have anecdotally observed that *P. ochraceus* specimens in central California were more challenging to remove from rocks after the wasting outbreak relative to before (MND, LMS, pers. comm. [though others have not remarked on this]), consistent with a hypothesis that those in more wave-exposed areas survived disproportionately (Fig. 7). These observations warrant further investigation into hypotheses about the roles of microenvironment and ecotypic variation in modulating SSW and will benefit from better characterization of microenvironments (Bell and Denny, 1994; Helmuth and Denny, 2003; Hata, 2015) as well as the leveraging of whole-genome sequencing and gene ontologies to distinguish between immune, temperature, and oxygen stress responses.

Integration: biology and environment across scales

The apparent alignment between small- and large-scale studies associating increased temperature and decreased wave exposure (or increased stratification and related effects, possibly also mediated by freshwater input) with an increased risk of SSW are intriguing. These factors are among or related to those known to shape sea star species' distributions (depth, temperature, salinity, and habitat; Hemery *et al.*, 2016) and communities (tidewater glacial presence, fetch, and tidal range; Konar *et al.*, 2019). They are among a handful of abiotic characteristics that have been previously associated with SSW (sea surface temperature, productivity, upwelling, wave energy, freshwater discharge; Eisenlord *et al.*, 2016; Kohl *et al.*, 2016; Menge *et al.*, 2016; Hewson *et al.*, 2018; Harvell *et al.*, 2019), and our narrative exploration emphasizes the subset highlighted here as having the most credible associations with SSW. This is also consistent with recent results that indicate that including SST in models of SSW yields more realistic dynamics (Aalto *et al.*, 2020) and with temperature being a hypothesized major factor controlling the onset and severity of disease outbreaks in both marine and terrestrial environments (Harvell *et al.*, 2002; Boyett *et al.*, 2007; Bruno *et al.*, 2007; Kilpatrick *et al.*, 2008; Burge *et al.*, 2014; Giraldo-Ospina *et al.*, 2020). The relative roles of chronic and acute heating remain underexplored.

Moreover, while the factors shaping species distributions and communities vary across depths, variations in the major risk factors of temperature, wave exposure and/or stratification, and freshwater input are concentrated on taxa occurring in the shallowest habitats that already experience the greatest extremes and expose organisms to stress (Petes *et al.*, 2008; Fly *et al.*, 2012; Monaco *et al.*, 2015). Thus, shallow-water species—such as *Asterias* spp. and *Heliaster kubiniji*, notably—are particularly at risk, as implicated in PCA analyses (Fig. 8) and consistent with one of the most substantial prior reports of SSW and translocation experiments in the Gulf of California (Dungan *et al.*, 1982).

Many genera of sea stars inhabit shallow waters, and likewise the group of species that exhibited SSW is polyphyletic (Schiebelhut *et al.*, 2022b). Perhaps consequently, there are few life-history or other ecological characteristics that associate with SSW (Fig. 8). In some cases, such as *Pisaster*, it may be difficult to tease shared ecological and life-history effects apart from a phylogenetic signal. However, depth distribution (or partial correlates thereof, *e.g.*, reproductive season; Fig. 8) appears implicated as a key trait by the contrast between *Pycnopodia*, a heavily affected shallow-water species, and *Rathbunaster*, its apparently unaffected deeper-water sister taxon. Given that SSW appears mediated *via* the water (DelSesto, 2015; Kohl *et al.*, 2016) and risk of developing symptoms ("infection") was positively associated with geographic proximity (Moritsch, 2018), oceanographic mechanisms—for example, unidirectional flow from deep to shallow waters *via* upwelling—may protect deeper-water species from SSW outbreaks in shallower-water taxa. This in turn suggests that apparent decreases in deepwater species abundances in 2013 and 2019 are indirect rather than direct connections to surface events—unless the marked downwelling in 2015–2017 could carry SSW deeper—highlighting the need to understand more about the potential roles of oceanographic and environmental distances (anomalies, critical points, and gradients) in the risk of infection.

The role of oceanography and environment, and their interaction with biology, also will be key to understanding patterns of recovery, which differed greatly among species. A simple prediction is that recovery should be related to life-history attributes (Schiebelhut *et al.*, 2022a). However, the >5-year-long failure of the fecund, planktotrophic, long pelagic larval–duration *P. helianthoides* to survive post-settlement at sites in Washington or to recolonize previously inhabited territory in Oregon and California is an enigma that contrasts with the relatively rapid recovery of *P. ochraceus*. But these are only two examples of the suite of sea stars that were contributing to communities recovering gradually since 2014, until interrupted in 2019 and so a process that was still unfinished over 7 years after the 2013 outbreak of SSW.

Remaining Gaps in Understanding and Avenues for Future Study

Our broad, integrative, spatial, and taxonomic analyses using historical data have clarified seven aspects of the mid-2010s SSW outbreak: (1) it most clearly affected a little over a dozen predominantly shallow-water species, with another 15 indicated to be susceptible; (2) prevalence was as high as 80% during the peak and 35% subsequently, depending on species and location; despite (3) rapid population-level effects, (4) environmental and species variation protracted the outbreak, which lasted 2–3 years from onset until (5) diminishing to chronic background rates of ~2%; (6) recruitment began immediately in many species, though spatially heterogeneous; and (7) elevated SST, decreased wave exposure, and freshwater discharge in the north are the abiotic

stressors most associated with SSW (of those considered). These outcomes are agnostic of whether a pathogen is involved. Our analyses also raised the specter of declines of deeper-water species in 2013 and 2019. However, these analyses also have emphasized that detailed data on the biological, ecological, and environmental cause(s) and consequences of the mid-2010s SSW outbreak are limited in scope and almost solely retrospective. New studies, conducted since the epidemic subsided, can tell us directly only about the current episode of chronic exposure, which may be a complex of one or more causes and symptoms that may differ from the mid-2010s outbreak itself. Though analyses of additional historical data may further constrain probable scenarios—for example, might there have been effects of pollution (including novel compounds) in freshwater runoff, nearshore primary productivity, aragonite saturation and upwelling, or weather above the waterline—existing data may always be somewhat indeterminate regarding the abiotic and/or biotic factors and interactions that caused the outbreak in the northeastern Pacific, and the implications for other regions are uncertain (Supplementary Document 7). As a future with greater environmental means and extremes continues to unfurl, we find ourselves largely unable to predict risk or to establish preventative measures. If the frequency of extreme events increases, it seems highly likely that many species of sea stars may not possess the capacity to recover between events and therefore are at greater risk of population decline, ratcheting down to extirpation, locally, regionally, and globally.

Designing monitoring networks to fill the key knowledge gaps exposed by the mid-2010s outbreak, and apparent 2019 decline, is essential. Data collection should at least match the geographic and taxonomic spread of this study, though being more spatially and temporally intensive would be useful; monitoring needs to be quantitative and include abiotic and biotic measurements, including observations of SSW. Community science surveys can help increase the intensity of observations, especially using a standardized framework and building on scientific research infrastructure to better address knowledge gaps (Supplementary Document 7). To the extent that measurement can be automated and synchronized on the finest scales at multiple locations chosen for specific comparisons and contrasts, we will gain greater insight complementing existing large-scale arrays. To the extent that measurements can occur consistently during nonoutbreak conditions, we can shed light on "normal" dynamics, which are the indispensable context for abnormal (epidemic) dynamics. Also, conceptual clarification will be needed to interpret increasing data. For example: How does the frequency of sampling interact with sea star growth rates to determine criteria for identifying recruits? Does a half century of global change shift baseline expectations of what constitutes an extreme event? Does the sequencing of events bias assumptions of cause and effect? And how should we make predictions if emerging conditions have no prior analog? To the extent that incoming data can be automatically analyzed and appropriately modeled to provide managers with simple, reliable indices of population dynamics and disease risk, we can facilitate more effective action.

A biogeographically cognizant ecoenvironmental study will deliver answers to what now seem prophetic observations from the 1970s: that similar die-offs in distinct regions indicate a common cause and rule out most kinds of localized disturbance as potential explanations, that biases exist in data availability for different taxa, and that there is a dearth of information on marine pathogens (Dungan *et al.*, 1982). Moreover, such a study will address basic questions in biology, ecology, and community ecology of sea stars, including the extent to which spatial synchrony is driven by environmental change *versus* dispersal or biotic interactions (Dallas *et al.*, 2020). Addressing questions of gene flow, adaptation, and drift in metapopulations will require a genomic framework (*e.g.*, Carroll *et al.*, 2020) that will benefit from developments in genomic monitoring (Cordier *et al.*, 2021), the potential of which has already been shown in enabling "genomic autopsy" of SSW (Ruiz-Ramos *et al.*, 2020). Until these steps are implemented and we understand usual levels of background variation, and until—and perhaps even beyond—the next outbreak, we may unavoidably need to remain somewhat agnostic about the unusual circumstances surrounding the mid-2010s SSW outbreak and concerned about the future.

Acknowledgments

We thank Ocean Wise and Andy Lamb for additional data provided by Donna Gibbs of Ocean Wise Conservation Association. Sarah Gravem was instrumental in tracking down datasets and contacts. Data from the northern Gulf of Alaska were collected by the Gulf Watch Alaska Program, which is funded by the *Exxon Valdez* Oil Spill Trustee Council. Data from the Center for Alaskan Coastal Studies (CACS) in Kachemak Bay, Alaska, was collected by a variety of community volunteers, youth groups, K–12 classes, and college groups as well as interns and CACS naturalist educators; we are grateful for their contributions. Pete Raimondi helped design aspects of this study, using data collected by the Multi-Agency Rocky Intertidal Network (MARINe): a long-term ecological consortium funded and supported by many groups. Please visit http://www.pacificrockyintertidal.org for a complete list of the MARINe partners responsible for monitoring and funding these data. Data management has been primarily supported by the Bureau of Ocean Energy Management, National Parks Service, the David and Lucile Packard Foundation, and US Navy. We acknowledge the Northwest Fisheries Science Center's Fisheries Resource Survey Team, as well as the captains, crew, and many volunteers who staffed National Marine Fisheries Service surveys between 2006 and 2019.

Samuel Winter kindly provided data on wave characteristics for Figure 7. We are grateful to Marm Kilpatrick, Sarah Gravem, Benjamin Miner, Ian Hewson, and Bruce Menge for perspectives on SSW, disease, and related matters previous to and/or during the workshops. Heather Coletti, John Pearse, Barbara Ralston, Eric Sanford, Ben Weitzman, and an anonymous reviewer provided comments that improved the manuscript; all errors remain our own. Any use of trade, firm, or product names is for descriptive purposes only and does not imply endorsement by the US government. The virtual workshop supporting development of this project and participation of JPW, MND, LMS, PJD, and P. T. Raimondi (University of California, Santa Cruz) was funded by National Science Foundation grants OCE-1737091, OCE-1737381, OCE-1737372, and OCE-1737127. RC was supported by Portuguese national funds from Foundation for Science and Technology (FCT) through project UIDB/04326/2020. Study design: MND, JPW, LMS, JLL. Execution of research and analyses: BK, RBL, MND, PJD, MG, KLB, LMS, AK, RC, CE-S, JLL, CMM, MST, KAG, JL, MMM, SBT. Manuscript preparation: MND, PJD, MG, JPW, LMS, RC, CMM, MMM, KAG, BK, KLB, RB-L, JLL, SAN, CE-S, SBT, MST. All authors approve this version and accept accountability for the authenticity of the study.

Literature Cited

Aalto, E. A., K. D. Lafferty, S. H. Sokolow, R. E. Grewelle, T. Ben-Horin, C. A. Boch, P. T. Raimondi, S. J. Bograd, E. L. Hazen, M. G. Jacox *et al.* 2020. Models with environmental drivers offer a plausible mechanism for the rapid spread of infectious disease outbreaks in marine organisms. *Sci. Rep.* **10:** 5975.

Aquino, C. A., R. M. Besemer, C. M. DeRito, J. Kocian, I. R. Porter, P. T. Raimondi, J. E. Rede, L. M. Schiebelhut, J. P. Sparks, J. P. Wares *et al.* 2021. Evidence that microorganisms at the animal-water interface drive sea star wasting disease. *Front. Mar. Sci.* **11:** 610009.

Bates, A. E., B. J. Hilton, and C. D. G. Harley. 2009. Effects of temperature, season and locality on wasting disease in the keystone predatory sea star *Pisaster ochraceus*. *Dis. Aquat. Org.* **86:** 245–251.

Beas-Luna, R., F. Micheli, C. B. Woodson, M. Carr, D. Malone, J. Torre, C. Boch, J. E. Caselle, M. Edwards, J. Freiwald *et al.* 2020. Geographic variation in responses of kelp forest communities of the California Current to recent climatic changes. *Glob. Change Biol.* ***26:*** 6457–6473.

Bell, E. C., and M. W. Denny. 1994. Quantifying "wave exposure": a simple device for recording maximum velocity and results of its use at several field sites. *J. Exp. Mar. Biol. Ecol.* ***181:*** 9–29.

Boyett, H. V., D. G. Bourne, and B. L. Willis. 2007. Elevated temperature and light enhance progression and spread of black band disease on staghorn corals of the Great Barrier Reef. *Mar. Biol.* **151:** 1711–1720.

Bruno, J. F., E. R. Selig, K. S. Casey, C. A. Page, B. L. Willis, C. D. Harvell, H. Sweatman, and A. M. Melendy. 2007. Thermal stress and coral cover as drivers of coral disease outbreaks. *PLoS Biol.* **5:** 1220–1227.

Bucci, C., M. Francoeur, J. McGreal, R. Smolowitz, V. Zazueta-Novoa, G. M. Wessel, and M. Gomez-Chiarri. 2017. Sea star wasting disease in *Asterias forbesi* along the Atlantic coast of North America. *PLoS One* **12:** e0188523.

Burge, C. A., C. M. Eakin, C. S. Friedman, B. Froelich, P. K. Hershberger, E. E. Hofmann, L. E. Petes, K. C. Prager, E. Weil, B. L. Willis *et al.* 2014. Climate change influences on marine infectious diseases: implications for management and society. *Annu. Rev. Mar. Sci.* **6:** 249–277.

Carroll, E. L., A. Hall, M. T. Olsen, A. B. Onoufriou, O. E. Gaggiotti, and D. J. F. Russell. 2020. Perturbation drives changing metapopulation dynamics in a top marine predator. *Proc. R. Soc. B* **287:** 20200318.

Cordier, T., L. Alonso-Sáez, L. Apothéloz-Perret-Gentil, E. Aylagas, D. A. Bohan, A. Bouchez, A. Chariton, S. Creer, L. Frühe, F. Keck *et al.* 2021. Ecosystems monitoring powered by environmental genomics: a review of current strategies with an implementation roadmap. *Mol. Ecol.* **30:** 2937–2958.

Cornwall, W. 2019. A new "blob" menaces Pacific ecosystems. *Science* **365:** 1233–1233.

Dallas, T. A., L. H. Antão, P. Juha, L. Reima, and O. Ovaskainen. 2020. Spatial synchrony is related to environmental change in Finnish moth communities. *Proc. R. Soc. B* **287:** 20200684.

Dean, T. A., and J. L. Bodkin. 2011. *SOP for Sampling of Intertidal Invertebrates and Algae on Sheltered Rocky Shores*, Ver. 4.6. Natural Resource Report NPS/SWAN/NRR—2011/397. Southwest Alaska Inventory and Monitoring Network, Anchorage.

Dean, T. A., J. L. Bodkin, and H. A. Coletti. 2014. *Protocol Narrative for Nearshore Marine Ecosystem Monitoring in the Gulf of Alaska*, Ver. 1.1. Natural Resource Report NPS/SWAN/NRR—2014/756. US National Park Service Natural Resource Stewardship and Science, Fort Collins, CO.

DelSesto, C. J. 2015. Assessing the pathogenic cause of sea star wasting disease in *Asterias forbesi* along the East Coast of the United States. MS thesis, University of Rhode Island, Kingston.

Dungan, M. L., T. E. Miller, and D. Thomson. 1982. Catastrophic decline of a top carnivore in the Gulf of California rocky intertidal zone. *Science* **216:** 989–991.

Eckert, G. L., J. M. Engle, and D. J. Kushner. 2000. Sea star disease and population declines at the Channel Islands. *Proc. Fifth Calif. Isl. Symp. US Miner. Manag. Serv.* **5:** 390–393.

Eisenlord, M. E., M. L. Groner, R. M. Yoshioka, J. Elliott, J. Maynard, S. Fradkin, M. Turner, K. Pyne, N. Rivlin, R. van Hooidonk *et al.* 2016. Ochre star mortality during the 2014 wasting disease epizootic: role of population size structure and temperature. *Philos. Trans. R. Soc. B* **371:** 20150212.

Fifer, J., B. Bentlage, S. Lemer, A. G. Fujimura, M. Sweet, and L. J. Raymundo. 2021. Going with the flow: how corals in high-flow environments can beat the heat. *Mol. Ecol.* **30:** 2009–2024.

Fly, E. K., C. J. Monaco, S. Pincebourde, and A. Tullis. 2012. The influence of intertidal location and temperature on the metabolic cost of emersion in *Pisaster ochraceus*. *J. Exp. Mar. Biol. Ecol.* **422–423:** 20–28.

Frankson, R., L. E. Stevens, K. E. Kunkel, S. M. Champion, D. R. Easterling, W. Sweet, and M. Anderson. 2022. *California State Climate Summary 2022.* NOAA Technical Report NESDIS 150-CA. National Oceanic and Atmospheric Administration/National Environmental Satellite, Data, and Information Service, Silver Spring, MD.

Fuess, L. E., M. E. Eisenlord, C. J. Closek, A. M. Tracy, R. Mauntz, S. Gignoux-Wolfsohn, M. M. Moritsch, R. Yoshioka, C. A. Burge, C. D. Harvell *et al.* 2015. Up in arms: immune and nervous system response to sea star wasting disease. *PLoS One* **10:** e0133053.

Giraldo-Ospina, A., G. A. Kendrick, and R. K. Hovey. 2020. Depth moderates loss of marine foundation species after an extreme marine heatwave: Could deep temperate reefs act as a refuge? *Proc. R. Soc. B* **287:** 20200709.

Gravem, S. A., W. N. Heady, V. R. Saccomanno, K. F. Alvstad, A. L. M. Gehman, T. N. Frierson, and S. L. Hamilton. 2021. *Pycnopodia helianthoides* (amended version of 2020 assessment). [Online]. IUCN Red List of Threatened Species. Available: https://www.iucnredlist.org/species/178290276/197818455 [2023, December 18].

Hamilton S. L., V. R. Saccomanno, W. N. Heady, A. L. Gehman, S. I. Lonhart, R. Beas-Luna, F. T. Francis, L. Lee, L. Rogers-Bennett, A. K. Salomon *et al.* 2021. Disease-driven mass mortality event leads to widespread extirpation and variable recovery potential of a marine predator across the eastern Pacific. *Proc. R. Soc. B* **288:** 20211195.

Harvell, C. D., C. E. Mitchell, J. R. Ward, S. Altizer, A. P. Dobson, R. S. Ostfeld, and M. D. Samuel. 2002. Climate warming and disease risks for terrestrial and marine biota. *Science* **296:** 2158–2162.

Harvell, C. D., D. Montecino-Latorre, J. M. Caldwell, J. M. Burt, K. Bosley, A. Keller, S. F. Heron, A. K. Salomon, L. Lee, O. Pontier *et al.* 2019. Disease epidemic and a marine heat wave are associated with the continental-scale collapse of a pivotal predator (*Pycnopodia helianthoides*). *Sci. Adv.* **5:** eaau7042.

Hata, T. 2015. Measuring and recreating hydrodynamic environments at biologically relevant scales. PhD diss., Stanford University, Stanford, CA.

Hayne, K. J., and A. R. Palmer. 2013. Intertidal sea stars (*Pisaster ochraceus*) alter body shape in response to wave action. *J. Exp. Biol.* **216:** 1717–1725.

Helmuth, B. S., and M. W. Denny. 2003. Predicting wave exposure in the rocky intertidal zone: Do bigger waves always lead to larger forces? *Limnol. Oceanogr.* **48:** 1338–1345.

Hemery, L. G., S. R. Marion, C. G. Romsos, A. L. Kurapov, and S. K. Henkel. 2016. Ecological niche and species distribution modelling of sea stars along the Pacific Northwest continental shelf. *Divers. Distrib.* **22:** 1314–1327.

Hewson, I., J. B. Button, B. M. Gudenkauf, B. Miner, A. L. Newton, J. K. Gaydos, J. Wynne, C. L. Groves, G. Hendler, M. Murray *et al.* 2014. Densovirus associated with sea-star wasting disease and mass mortality. *Proc. Natl. Acad. Sci. USA* **111:** 17278–17283

Hewson, I., K. S. I. Bistolas, E. M. Quijano Cardé, J. B. Button, P. J. Foster, J. M. Flanzenbaum, J. Kocian, C. K. Lewis. 2018. Investigating the complex association between viral ecology, environment, and northeast Pacific sea star wasting. *Front. Mar. Sci.* **5:** 77.

Hewson, I., B. Sullivan, E. W. Jackson, Q. Xu, H. Long, C. Lin, C. E. M. Quijano, J. Seymour, N. Siboni, M. R. L. Jones *et al.* 2019. Something old, something new? Review of wasting and other mortality in Asteroidea (Echinodermata). *Front. Mar. Sci.* **6:** 406.

Huey, R. B., and P. R. Grant. 2020. Lizards, toepads, and the ghost of hurricanes past. *Proc. Natl. Acad. Sci. USA* **117:** 11194–11196.

Jaffe, N., R. Eberl, J. Bucholz, and C. S. Cohen. 2019. Sea star wasting disease demography and etiology in the brooding sea star *Leptasterias* spp. *PLoS One* **14:** e0225248.

Kassambara, A., and F. Mundt. 2020. Factoextra: extract and visualize the results of multivariate data analyses. [Online]. CRAN R package ver. 1.0.7. Available: https://CRAN.R-project.org/package=factoextra [2022, September 19].

Keller, A. A., J. R. Wallace, and R. D. Methot. 2017. *The Northwest Fisheries Science Center's West Coast Groundfish Bottom Trawl Survey: Survey History, Design, and Description*. NOAA TechMemo NMFS-NWFSC-136. National Oceanic and Atmospheric Administration, Washington, DC.

Kelley, D., and C. Richards. 2021. oce: analysis of oceanographic data. [Online]. R package version 1.4-0.

Available: https://CRAN.R-project.org/package=oce [2022, March 13].

Kilpatrick, A. M., M. A. Meola, R. M. Moudy, and L. D. Kramer. 2008. Temperature, viral genetics, and the transmission of West Nile virus by *Culex pipiens* mosquitoes. *PLoS Pathog.* **4:** e1000092.

Kohl, W. T., T. I. McClure, and B. G. Miner. 2016. Decreased temperature facilitates short-term sea star wasting disease survival in the keystone intertidal sea star *Pisaster ochraceus*. *PLoS One* **11:** e0153670.

Konar, B., T. J. Mitchell, K. Iken, H. Coletti, T. Dean, D. Esler, M. Lindeberg, B. Pister, and B. Weitzman. 2019. Wasting disease and static environmental variables drive sea star assemblages in the Northern Gulf of Alaska. *J. Exp. Mar. Biol. Ecol.* **520:** 151209.

Kucheryavskiy, S. 2020. mdatools: R package for chemometrics. *Chemometr. Intel. Lab. Syst.* **198:** 103937.

Lê, S., J. Josse, and F. Husson. 2008. FactoMineR: a package for multivariate analysis. *J. Stat. Softw.* **25:** 1–18.

Legendre, P., and L. F. Legendre. 2012. *Numerical Ecology*. Elsevier, Amsterdam.

MARINe (Multi-Agency Rocky Intertidal Network). 2015. Time lapse: sea star wasting syndrome. [Online]. University of California, Santa Cruz. Available: http://www.eeb.ucsc.edu/pacificrockyintertidal/data-products/sea-star-wasting/time-lapse.html [2018, August 20].

MARINe. 2018. Sea star species affected by wasting syndrome. [Online]. Available: https://marine.ucsc.edu/data-products/sea-star-wasting/species_affected_2018_0920.pdf [2023, October 23].

McPherson, M. L., D. J. I. Finger, H. F. Houskeeper, T. W. Bell, M. H. Carr, L. Rogers-Bennett, and R. M. Kudela. 2021. Large-scale shift in the structure of a kelp forest ecosystem co-occurs with an epizootic and marine heatwave. *Commun. Biol.* **4:** 298.

Menge, B. A., E. B. Cerny-Chipman, A. Johnson, J. Sullivan, S. Gravem, and F. Chan. 2016. Sea star wasting disease in the keystone predator *Pisaster ochraceus* in Oregon: insights into differential population impacts, recovery, predation rate, and temperature effects from long-term research. *PLoS One* **11:** e0153994.

Miner, C. M., J. L. Burnaford, R. F. Ambrose, L. Antrim, H. Bohlmann, C. A. Blanchette, J. M. Engle, S. C. Fradkin, R. N. Gaddam, C. D. G. Harley *et al.* 2018. Large-scale impacts of sea star wasting disease (SSWD) on intertidal sea stars and implications for recovery. *PLoS One* **13:** e0192870.

Monaco, C. J., D. S. Wethey, S. Gulledge, and B. Helmuth. 2015. Shore-level size gradients and thermal refuge use in the predatory sea star *Pisaster ochraceus*: the role of environmental stressors. *Mar. Ecol. Prog. Ser.* **539:** 191–205.

Montecino-Latorre, D., M. E. Eisenlord, M. Turner, R. Yoshioka, C. D. Harvell, C. V. Pattengill-Semmens, J. D. Nichols, and J. K. Gaydos. 2016. Devastating transboundary impacts of sea star wasting disease on subtidal asteroids. *PLoS One* **11:** e0163190.

Moritsch, M. 2018. Ecological causes and consequences of sea star wasting syndrome on the Pacific Coast. PhD thesis, University of California, Santa Cruz.

O'Reilly, W. C., C. B. Olfe, J. Thomas, R. J. Seymour, and R. T. Guza. 2016. The California coastal wave monitoring and prediction system. *Coast. Eng.* **116:** 118–132.

Orr, J. A., R. D. Vinebrooke, M. C. Jackson, K. J. Kroeker, R. L. Kordas, C. Mantyka-Pringle, P. J. Van den Brink, F. De Laender, R. Stoks, M. Holmstrup *et al.* 2020. Towards a unified study of multiple stressors: divisions and common goals across research disciplines. *Proc. R. Soc. B* **287:** 20200421.

Oulhen, N., M. Byrne, P. Duffin, M. Gomez-Chiarri, I. Hewson, J. Hodin, B. Konar, E. K. Lipp, B. G. Miner, A. L. Newton *et al.* 2022. A review of asteroid biology in the context of sea star wasting: possible causes and consequences. *Biol. Bull.* **243**: 50–75.

Pebesma, E. 2018. Simple features for R: standardized support for spatial vector data. *R J.* **10:** 439–446.

Pespeni, M. H., and M. M. Lloyd. 2023. Sea stars resist wasting through active immune and collagen systems. *Proc. R. Soc. B* **290:** 2902023034720230347.

Petes, L. E., M. E. Mouchka, R. H. Milston-Clements, T. S. Momoda, and B. A. Menge. 2008. Effects of environmental stress on intertidal mussels and their sea star predators. *Oecologia* **156:** 671–680.

Rasmussen, L. L., M. L. Carter, R. E. Flick, M. Hilbern, J. T. Fumo, B. D. Cornuelle, B. K. Gordon, L. F. Bargatze, R. L. Gordon, and J. A. McGowan. 2020. A century of Southern California coastal ocean temperature measurements. *J. Geophys. Res. Ocean* **125:** e2019JC015673.

R Core Team. 2020. R: a language and environment for statistical computing. [Online]. R Foundation for Statistical Computing, Vienna. Available: http://www.R-project.org [2022, March 23].

Ruiz-Ramos, D. V., L. M. Schiebelhut, K. J. Hoff, J. P. Wares, and M. N Dawson. 2020. Initial comparative genomic autopsy of wasting disease in sea stars. *Mol. Ecol.* **29:** 1087–1102.

Schiebelhut, L. M., J. B. Puritz, and M. N Dawson. 2018. Decimation by sea star wasting disease and rapid genetic change in a keystone species, *Pisaster ochraceus*. *Proc. Natl. Acad. Sci. USA* **115:** 7069–7074.

Schiebelhut, L. M., B. Gaylord, R. K. Grosberg, L. J. Jurgens, and M. N Dawson. 2022a. Species' attributes predict the relative magnitude of ecological and genetic recovery following mass mortality. *Mol. Ecol.* **31:** 5714–5728.

Schiebelhut, L. M., M. Giakoumis, R. Castilho, P. J. Duffin, V. E. Garcia, J. B. Puritz, J. P. Wares, G. M. Wessel, and M. N Dawson. 2022b. Is it in the stars? Exploring the relationships between species' traits and sea star wasting disease. *Biol. Bull.* **243:** 315–327.

Suryan, R. M., M. L. Arimitsu, H. A. Coletti, R. R. Hopcroft, M. R. Lindeberg, S. J. Barbeaux, S. D. Batten, W. J. Burt, M. A. Bishop, J. L. Bodkin *et al.* 2021. Ecosystem response persists after a prolonged marine heatwave. *Sci. Rep.* **11:** 6235.

USGS Alaska Science Center, National Park Service Southwest Alaska Inventory and Monitoring Network. 2022. *Rocky Intertidal Data from Prince William Sound, Katmai National Park and Preserve, and Kenai Fjords National Park*. US Geological Survey data release. US Geological Survey and National Park Service, Washington, DC.